

October 18, 2012



PP-012-016

A Computer Algorithm For Engineering Off-Shell Multiplets With Four Supercharges On The World Sheet

Keith Burghardt¹, and S. James Gates, Jr.²

*Center for String and Particle Theory
Department of Physics, University of Maryland
College Park, MD 20742-4111 USA*

ABSTRACT

We present an adinkra-based computer algorithm implemented in a Mathematica code and use it in a limited demonstration of how to engineer off-shell multiplets with four supercharges on the world sheet. Using one of the outputs from this algorithm, we present evidence for the unexpected discovery of a previously unknown 8 - 8 representation of $\mathcal{N} = 2$ world sheet supersymmetry. As well, we uncover a menagerie of $(p, q) = (3, 1)$ world sheet supermultiplets.

¹keith@umd.edu

²gatess@wam.umd.edu

1 Introduction

Historically, there have been two approaches used for the discovery of off-shell supersymmetrical multiplets and these are:

- (a.) the component method, and
- (b.) the superfield method.

The former dates to the earliest realizations of supersymmetrical representations [1]. It relies on intuition to make well-motivated guesses as to the field content of a supermultiplet and these are verified by checking for the closure of a set of SUSY variations. The latter dates to introduction of superfields [2]. In this method, one relies on intuition to make well-motivated guesses as the structure of a set of super-differential equations to define an irreducible off-shell multiplet.

The use of intuition and guesses in both of these methods is indicative of a need for a comprehensive theory of off-shell linear representations of supersymmetry.

It is the purpose of this work to introduce a new and third method for the discovery of off-shell linear supersymmetrical representations. In the new approach, intuition and guesses are replaced by a computer-enabled search of the 1D zoo of off-shell linear supersymmetrical representations provided by adinkras [3]. In the following, we will describe an approach that relies on recent advances in understanding the relation of adinkras to supersymmetrical field theories on the world sheet in order to create an algorithm. It is capable of systematically scanning the adinkra zoo for representations that can be lifted to 2D theories. Initially, this was undertaken to simply validate this approach in a small domain of adinkras. Quite unexpectedly, we seem to have found a new representation. If this interpretation stands up to additional investigation, it will mark the first time a new off-shell linear representation has been discovered by a systemic deductive means..

Adinkras have been shown to completely describe off-shell one dimensional linear realizations of supersymmetry in graphical form. However, we have long argued [4] that their applicability extends to \mathcal{N} -extended supersymmetrical representations in all dimensions. The basis for this suggestion is the proposal that adinkras are to off-shell supersymmetric representation theory as $SU(3)$ weight space diagrams are to hadronic representations. It is well known that $SU(3)$ weight space diagrams do not just apply to the fundamental representations, but to all representations.

It was predicted in the work of Ref. [4] that there must exist a property of “SUSY holography” by which higher dimensional off-shell SUSY representations are holo-

graphically stored in the representation theory of one dimensional SUSY quantum mechanical systems. In other words, adinkras must be holograms for higher dimensional SUSY representations.

The first actual demonstration of this property was shown in the work of Ref. [5], where a logically consistent mathematical manner for doing so was presented in some examples. Furthermore, a set of requirements for dimensional extensions more generally were given. However, this approach is computationally demanding as it basically requires checks of compatibility between equations.

Quite recently and using entirely different methods [6], it was shown how 1D $\mathcal{N} = 4$ valise adinkras holographically encode the data required to reconstruct the $(1, 3)$ Clifford bundle required for four dimensional fermions in some 4D, $\mathcal{N} = 1$ supermultiplets. As valise adinkras form the simplest of one dimensional supersymmetric representations, this observation diminishes some of the effort surrounding node-raising analysis in the work of Ref. [5]. This will be discussed in a specific result at the end of chapter six.

The search for computationally efficient methods for the derivation, from adinkra-based descriptions, of SUSY multiplets in greater than one dimension continued. This resulted in Ref. [7], which found that a special class of paths (known as “two-color ambidextrous bow ties” - see Fig. # 1) within adinkras act as obstructions to their extension from one dimensional to two dimensional systems.

We believe the work of Ref. [7] will stand any challenge to the idea that SUSY holography exists, at least in the case of going from one to two bosonic dimensions. As off-shell two dimensional SUSY representations are contained within four dimensional SUSY representations, work showing dimensional extension from one to two dimensions also supports the contention about SUSY holography more generally.

With the discovery of the “no two-color ambidextrous bow tie” theorem there now exists a proof that adinkras have been shown to be holograms for off-shell two dimensional linear realizations of supersymmetry.

The absence of these special “two-color ambidextrous bow tie” paths acts as a filter. A problem has remained, however, on how to efficiently determine whether adinkras are liftable without having to visually inspect 2-color paths in adinkras looking for the obstructive paths. This is due to the sheer number of paths through which one needs to search.

In this work, we present an efficient algorithm which can determine liftability for arbitrary adinkras of arbitrary size, using two groups of matrices that we shall

introduce and call by the name “color matrices.” These will be denoted by the symbols \mathcal{B}_{1L} and \mathcal{B}_{1R} . These matrices are then used to construct “color block matrices,” \mathbf{C}_I , which describe the linear transformations on the entire vector space of bosons and fermions, $\Phi \oplus \Psi$ under the action of the D_1 super-differential operator.

We will show that multiplying two color matrices together, $\mathcal{B}_{1L}\mathcal{B}_{1R}$, can be used to count the number of bow ties for any two-color combination, (I, J) . Knowing whether bow ties exist for specific color combinations is all one needs to determine if adinkras have ambidextrous bow ties and are therefore non-liftable. In addition, we present results concerning the dimensional extension of 1D adinkras to 2D adinkras based on the tesseract adinkra and code-folded tesseract adinkra. These results will demonstrate the utility of this algorithm. This gives an explicit path by which one can start solely with adinkras and no other information to engineer the equations for off-shell supermultiplets on the world sheet.

The paper is organized as follows: in Section 2, we describe the different types of liftable and non-liftable two-color paths. In Section 3, we review the Bow Tie Theorem in Ref. [7], and bow tie graphs, which we use to determine liftability of the adinkra. In Section 4, we introduce the liftability algorithm, and the color matrices, which are essential to determine liftability. In Section 5, we give a discussion on why adding the notion of helicity to one dimensional adinkras triggers the need to introduce a second bosonic coordinate and, perhaps even more interesting, a Lorentzian structure for a world sheet. In Section 6, we describe the results of a search that demonstrate the algorithm’s usefulness by calculating which ambidextrous adinkras based on the tesseract adinkra and code-folded tesseract are liftable, This includes an enumeration. Our conclusions are given in Section 7. We include four appendices. In the first and second there are given the 2D SUSY equations (equivalent to SUSY variations) for two classes of liftable adinkras that correspond to the $\mathcal{GR}(2,2)$ and $\mathcal{GR}(4,4)$ algebras. The third appendix presents an evidence for one such adinkra is a previously unknown representation. The final appendix presents the Mathematica code used for the search for liftable adinkras.

2 On Bow Tie & Diamond Adinkras

No matter how many colors appear in an arbitrarily complicated adinkra, the work of Ref. [7] implies that only two-color closed paths are relevant to the dimensional extension of supersymmetrical representations from those that depend on a single bosonic coordinate to those that depend on two bosonic coordinates. There are

only two types of such paths as shown in Fig. # 1. The main difference between

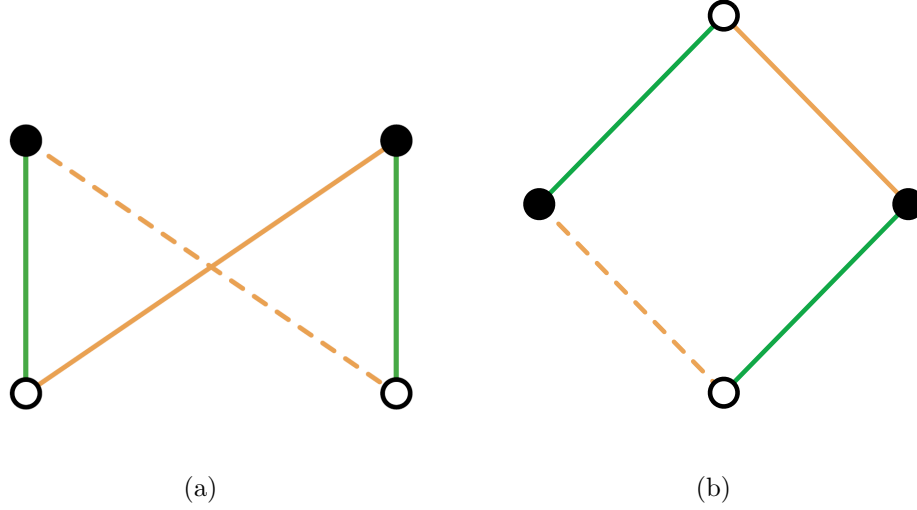


Figure 1: The bow tie two-color path (left) and the diamond two-color path (right).

one dimensional spinors and two dimensional spinors arises from the fact that only the latter possess a helicity, i. e. a two dimensional spinor can be ‘spin-up’ ($+\frac{1}{2}$) or ‘spin-down’ ($-\frac{1}{2}$). Operationally, this means that if one begins with a one dimensional spinor derivative operator, D_I , it may be regarded as having arisen from the projection of either D_{+I} or D_{-I} . So as a minimal requirement for extending from one dimensions to two dimensions, an operator $\text{Spin}(D_I)$ must be introduced. This operator assigns a value of the two-dimensional helicity (either D_{+I} or D_{-I}) to the one-dimensional spinor D_I .

Ambidextrous two-color bowtie adinkras are bowtie adinkras where the assignment of spin to the two distinct colors is such that one has spin up and the other has spin down. Unidextrous two-color bowtie adinkras are adinkras where the assignment of spin to the two distinct colors is such that both have either spin up or both have spin down. Ambidextrous and unidextrous bow ties look the same from the point of view of spinors in a space with a single bosonic dimension. In a space of two bosonic dimensions things change due to the operator $\text{Spin}(D_I)$.

For example, the diamond adinkra in Fig. # 1 under the action of all possible possible choices of the spin gives rise to the four graphs that we show in Fig. # 2. As the links in the first two of these adinkras are associated with both of the two possible spin states, they are ambidextrous. In the third and fourth adinkras. the links are associated solely with spin up (third adinkra) or solely with spin down

(fourth adinkra). Hence, they are unidextrous diamond adinkras.

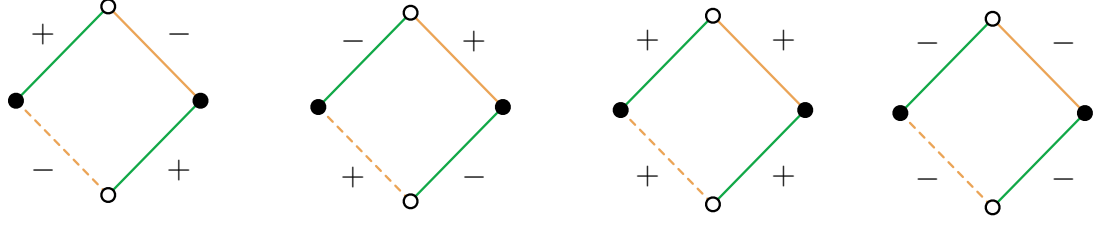


Figure 2: Ambidextrous and unidextrous diamond adinkras.

In a similar, manner the bow tie adinkra in Fig. # 1 under the action of all possible choices of the spin gives rise to four graphs below.

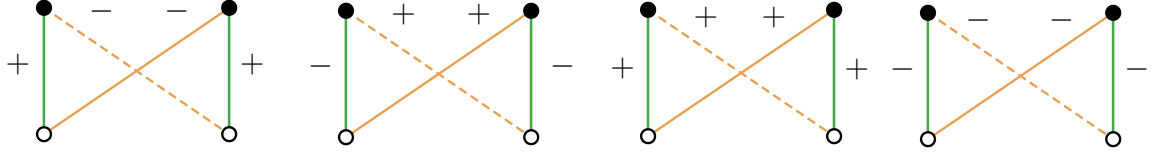


Figure 3: Ambidextrous (left) and unidextrous (right) bow tie adinkras.

It is the *a priori* appearance of the ambidextrous two-color bow tie adinkras (as in the two leftmost graphs above) that prevent such adinkras from describing supersymmetrical systems whose nodes depend on two bosonic coordinates. In adinkras of more colors, it is this subset of graphs that prevents such adinkras from describing supersymmetrical systems whose nodes are permitted to depend on two bosonic coordinates.

3 Liftability and Bow Ties

The Bow Tie Theorem [7] is based on the possibility of defining a graph theoretic quantity \mathcal{B}_N which is used to explicitly determine ‘liftability’ of two-color paths. The formal mathematical statement of the discussion in this chapter can all be found in the work of Ref. [7]. Here we will take a different track and approach this from arguments familiar to physicists.

Let us begin using physical analogies to understand the “Bow Tie Theorem.” We can imagine the images in Fig. # 1 represent electrical circuits. To answer the

question of the voltage difference measured across any node, it would suffice to use Kirchoff's Voltage Law. As an integral this takes the form

$$\mathcal{V} = - \oint \vec{\mathcal{E}} \cdot d\vec{\ell} \quad , \quad (1)$$

where the closed integral begins on one side of an infinitesimal node, is taken through the adjoining link, follows a path that ends up on the opposite of the side of the same node after traversing the circuit.

Next we make the replacements given by

$$\begin{aligned} \mathcal{V} &\longrightarrow \mathcal{B}_N \quad , \\ \oint \vec{\mathcal{E}} \cdot d\vec{\ell} &\longrightarrow - \sum_{links} \text{Spin}(\text{D}_1) (h_f - h_i) \quad . \end{aligned} \quad (2)$$

The first of these replaces the voltage by a quantity we may call the ‘‘Bow Tie Number’’ denoted by \mathcal{B}_N . In the second replacement, the integral is replaced by a sum over the links in a closed path. The paths that are relevant are two-color minimal length circuits in the adinkra and the links are chosen to correspond to this restriction. The differential line elements are replaced by the differences in heights ($h_f - h_i$) of the end points of the links along a path, and the electrical field is replaced by a function $\text{Spin}(\text{D}_1)$ which assigns values $\pm \frac{1}{2}$ to the D-operator associated with each link.

It is well known that given a capacitance C_0 , there is an associated energy

$$\mathcal{U} = \frac{1}{2} C_0 \left[\oint \vec{\mathcal{E}} \cdot d\vec{\ell} \right]^2 \quad , \quad (3)$$

but, we can use a second analogy to understand the significance of \mathcal{B}_N . Let us imagine a physical system where there is an interaction energy between a spin field $\vec{\mathcal{S}}$ and differential lattice vectors $d\vec{\ell}$ such that the energy takes the form

$$\mathcal{U} = \frac{1}{2} L_0 \left[\oint \vec{\mathcal{S}} \cdot d\vec{\ell} \right]^2 \quad . \quad (4)$$

A discretization of the integral immediately above, leads to an expression that is virtually the same as appears in (2) where the function $\text{Spin}(\text{D}_1)$ corresponds to the projection of the spin onto the differential lattice vectors. The quantity L_0 is introduced in order for the equation in (4) to possess the correct engineering dimensions.

For the two-color closed paths in Fig. # 1, the quantity \mathcal{B}_N can be explicitly expressed as

$$\mathcal{B}_N = h(\text{D})(\Delta h)_1 + h(\text{D})(\Delta h)_2 + h(\text{D})(\Delta h)_3 + h(\text{D})(\Delta h)_4 \quad , \quad (5)$$

and the colorful pre-factor symbols correspond to values of $\pm \frac{1}{2}$ depending on the choice of either spin-up or spin-down for the link of that color shown in Fig. # 1.

In order to complete the calculation of \mathcal{B}_N , the orientations of the spins must be specified.

The spin of the different colored links can either remain aligned (analogous to the ferromagnetic alignments of spins) or alternate between each adjacent links (analogous to the anti-ferromagnetic spin alignments). In the “ferromagnetic case” \mathcal{B}_N takes the form

$$\mathcal{B}_N = \pm \frac{1}{2} \{ (\Delta h)_1 + (\Delta h)_2 + (\Delta h)_3 + (\Delta h)_4 \} \quad , \quad (6)$$

and in the “anti-ferromagnetic case” \mathcal{B}_N takes the form

$$\mathcal{B}_N = \pm \frac{1}{2} \{ (\Delta h)_1 - (\Delta h)_2 + (\Delta h)_3 - (\Delta h)_4 \} \quad . \quad (7)$$

The third and fourth adinkras in Fig. # 1 and the third and fourth adinkras in Fig. # 2 correspond to the cases of “ferromagnetic” conditions. The first and second adinkras in Fig. # 1 and the first and second adinkras in Fig. # 2 correspond to the cases of “anti-ferromagnetic” conditions.

Under the “ferromagnetic” conditions, \mathcal{B}_N is zero for both bow tie and diamond adinkras. However, under the “anti-ferromagnetic” conditions, \mathcal{B}_N is zero for the diamond adinkra, but ± 1 for the bow tie adinkra³.

If we think of the adinkras in Fig. # 1 as the micro-states of an ensemble, then in the ferromagnetic regime both have the same energy as defined by (4). In the anti-ferromagnetic regime, only the diamond adinkra has the lowest energy. So the ‘ground state’ of the ensemble consists of all adinkras in Fig. # 2 and the unidextrous bow tie adinkras of figure Fig. # 3. No ambidextrous two-color bow tie adinkras exist in the ground state.

Whether a given one dimensional adinkra can be lifted to describe a two dimensional off-shell multiplet is found using the Bow Tie Theorem, which states that an adinkra of arbitrary complexity, possessing two-color bow tie paths, cannot be lifted to higher dimensions if it has non-vanishing Bow Tie Number.

Clearly, if all line colors were unidextrous, the adinkra would always be liftable. Determining whether “ambidextrous” adinkras are liftable is less trivial. For the rest of the paper, it is assumed we are lifting non-unidextrous adinkras.

For a given adinkra, instead of checking bow tie numbers directly, it is much

³As the differences in heights in an adinkra correspond to differences in the engineering dimensions of the fields related by a SUSY transformation, these changes in the values of h across a link correspond to $\pm 1/2$ and this leads to the stated values for \mathcal{B}_N .

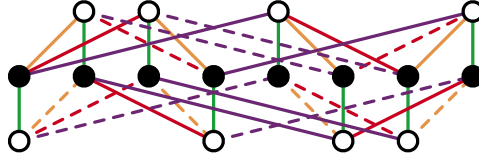


Figure 4: A liftable tesseract adinkra, with green lines that are bow tie free.

simpler to determine liftability by checking which colors form bow ties. As long as there are at least 2 sets of line colors that can have opposite spin values, while simultaneously remaining ambidextrous bow tie-free, the adinkra is liftable.

For example, in Fig. # 5, we see the valise adinkra can't be liftable because all the lines have bow ties. This can be symbolically shown in the “bow tie graph” in Fig. # 5(b), where each node represents a line color, while every line represents two-color bow ties between those two colors. As the graph shows, every color has bow ties with every other, therefore it is impossible not to create ambidextrous bow ties if the adinkra is non-unidextrous. For a general adinkra to be liftable, there must be at least two disconnected subgraphs, each of which separately have nodes with the same spin value to remove all ambidextrous bow ties.

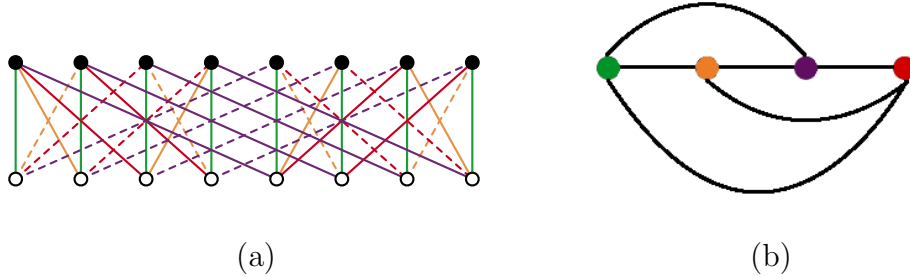


Figure 5: The unliftable ambidextrous valise adinkra (left) and bow tie graph (right).

A contrasting example appears in Fig. # 6 where we see an example of a liftable

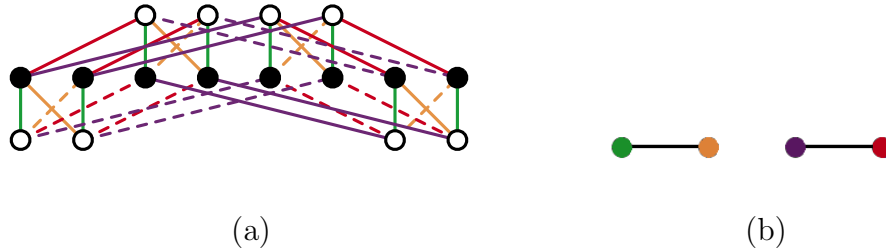


Figure 6: A liftable ambidextrous valise adinkra (left) and bow tie graph (right).

ambidextrous adinkra because the bow ties formed are green-yellow, as well as red-purple. Assigning “−” to the green and yellow lines, while assigning “+” to the red and purple lines allows the ambidextrous adinkra to remain liftable. This implies that the bow tie graph in Fig. # 6(b) has two disconnected sub-graphs.

If an adinkra is folded, it is unnecessary to look at every line color. Instead one only needs to inspect the “hypercubic” sub-adinkra (i. e. the underlying adinkra with lines topologically the same as edges on of a hypercube).

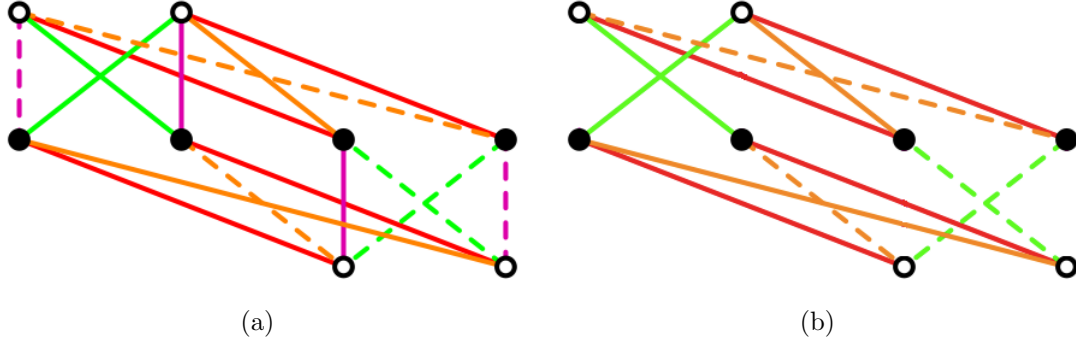


Figure 7: A chiral supermultiplet whose associated equations can lift to two dimensions (left), and a hypercubic sub-adinkra (right).

In Fig. # 7, the adinkra is liftable by assigning “+” to purple and green colors, while “−” to all other colors in the adinkra. All bow ties will be unidextrous, thereby preserving liftability.

We can, however, determine liftability of the folded adinkra on a subset of colored lines that can make the adinkra “hypercubic”, which reduces calculations, and simplifies the liftability algorithm because we can look at fewer lines. If we call one color “non-hypercubic” in Fig. # 7(a), such as the purple line, then the sub-adinkra made from 3 (hypercubic) lines is liftable because the green lines make bow ties with no other color, as seen in Fig. # 7(b). We claim that determining lift ability of the hypercubic sub-adinkra, determines liftability for the entire adinkra.

To prove this, however, we must first prove that hypercubic lines and non-hypercubic lines always form bow ties with each other in an adinkra.

Lemma 1 :

Non-hyperbolic lines always create bow ties with the hypercubic lines in an adinkra.

Proof :

Let us make a folded adinkra with only 1 designated non-hypercubic line color, and

r hypercubic line colors. Because the hypercubic lines are not unique, we can remove some 1 hypercubic line to re-create a hypercubic adinkra (forcing the non-hypercubic line to be part of a hypercubic adinkra). Because there are $r + 1$ nodes on the second row, but only r lines, the adinkra cannot be fully extended (i.e. must contain bow ties). If the non-hypercubic line doesn't create bow ties with those hypercubic lines, then we can add the previous hypercubic colored lines back into the adinkra, and take another hypercubic line color out. Doing this some finite number of times, we will always obtain non-hypercubic lines creating bow ties with hypercubic lines because the adinkra contains bow ties. If the non-hypercubic lines never created bow ties with the hypercubic lines, then we could create a fully extended hypercubic sub-adinkra which is impossible.

Now, let us assume this is true for a folded adinkra with $k - 1$ non-hypercubic lines, and r hypercubic lines such that $k \leq \frac{r!}{3!(r-1)!}$, the total number of non-hypercubic lines possible. Therefore, $r + k$ nodes connect to the $r + k$ lines for one of the top nodes which again. By again removing any $k - 1$ non-hypercubic lines, we find that the k^{th} non-hypercubic line makes bow ties with at least one other hypercubic line color by a similar argument to the one non-hypercubic line case.

□

Now we have the tools to prove the theorem. We will use the above lemma to show that, if ambidextrous bow ties always appear in hypercubic sub-adinkras, then adding non-hypercubic line colors will not make the adinkra liftable.

Theorem 1 : Hypercube Adinkra Liftability Theorem

The adinkra is liftable if and only if the adinkra's hypercubic lines contain no ambidextrous bow ties.

Proof :

Let us first assume the hypercubic lines contain ambidextrous bow ties. Because non-hypercubic lines create bow ties with hypercubic lines by Lemma 1, if the hypercubic lines contain ambidextrous bow ties, then by adding 1 non-hypercubic line, our only option to remove ambidextrous bow ties is to make the sign of all hypercubic lines $+1$ or -1 . If that is true, however, then the non-hypercubic line will have to have the opposite sign (in which case it creates an ambidextrous bow tie) or same sign, which is impossible. Therefore adding 1 non-hypercubic line doesn't make the adinkra liftable. If we add k hypercubic lines, then by Lemma 1, they too will cre-

ate bow ties with hypercubic lines, so by a similar argument, these cannot make the adinkra liftable.

Now let us go the other direction and assume the adinkra is not liftable. If the adinkra's hypercubic lines contain ambidextrous bow ties then we're done. If, however, the non-hypercubic lines contain ambidextrous bow ties, then all the non-hypercubic line have to be the same sign to remove their non-ambidextrous bow ties. because every non-hypercubic line has bow ties with hypercubic lines, all the lines must be the same sign to remove non-ambidextrous bow ties which is impossible. We can remove k hypercubic lines as before, and still find the adinkra is not liftable, because ambidextrous bow ties will still exist. Now, by the previous paragraph, we can add the k lines back and find that the non-hypercubic lines also create ambidextrous bow ties. By removing the k non-hypercubic lines, we then find that the hypercubic lines create ambidextrous bow ties, which finishes our proof.

□

4 Are Adinkras Deemed Liftable by Electric Shapes?

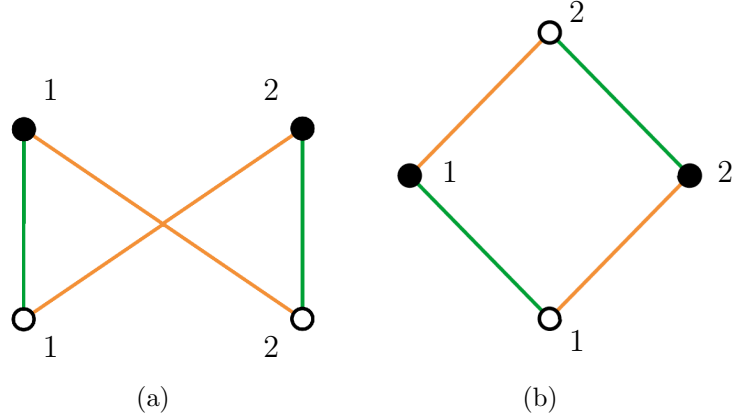


Figure 8: Bow tie and diamond two-color closed paths with line dashing removed.

Before we introduce the algorithm, we will introduce color matrices from which we can determine bow ties and diamonds.

The bow tie adinkra to the left in Fig. # 8 is called a “valise” and naturally leads to a lexicographic numbering of the nodes as shown (in this section we remove line dashing for clarity). The diamond adinkra on the right in Fig. # 8 is obtained from the bow tie adinkra by ‘lifting’ the bosonic 2 node on the lower right of the bow tie adinkra.

Color matrices are formed by decomposing an adinkra into its monochromatic components, as shown in Fig. # 9 for the bow tie, and in Fig. # 10 for the diamond. It is obvious in Fig. # 8 that the lines are topologically the same as the edges of a square. Once we've partitioned the set of line colors into k non-hypercubic colors, and $\mathcal{N} - k$ hypercubic colors, we can introduce parameters $\beta_I^{\pm 1}$, where "I" corresponds to the I^{th} hypercubic line color. We assign a value of β_I or β_I^{-1} depending on whether the colored line segment is above or below the node attached to it. The $\beta_i^{\pm 1}$ assigning is equivalent to multiplying a fermion or boson field, by 1 or ∂_τ in an associated equation within an adinkra, depending on whether the fermion or boson's associated node is above or below its superpartner.

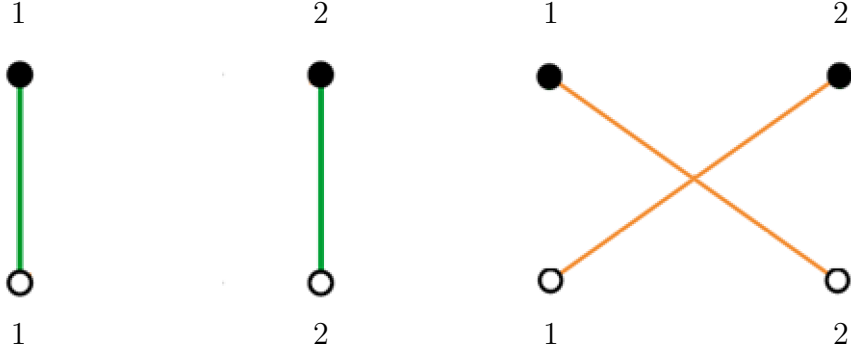


Figure 9: The β -parameter assignments to bow tie edges.

The numerical labels attached to each the nodes allows us to translate each diagram into a color matrix. We associate each bosonic nodal label with a row entry, and each fermionic nodal label with a column entry in the color matrix denoted \mathcal{B}_{1R} , while we associate each fermionic node label with a row and bosonic node label with a column in the matrix denoted \mathcal{B}_{1L} . Thus for the bow tie decomposition, shown in Fig. #9, the green color matrices are

$$\mathcal{B}_{1L} = \begin{pmatrix} \beta_1^{-1} & 0 \\ 0 & \beta_1^{-1} \end{pmatrix} , \quad \mathcal{B}_{1R} = \begin{pmatrix} \beta_1 & 0 \\ 0 & \beta_1 \end{pmatrix} , \quad (8)$$

while the yellow color matrices are

$$\mathcal{B}_{2L} = \begin{pmatrix} 0 & \beta_2^{-1} \\ \beta_2^{-1} & 0 \end{pmatrix} , \quad \mathcal{B}_{2R} = \begin{pmatrix} 0 & \beta_2 \\ \beta_2 & 0 \end{pmatrix} , \quad (9)$$

In comparison the green lines, for the diamond adinkra's color matrices, shown in Fig. #10 below, are

$$\mathcal{B}_{1L} = \begin{pmatrix} \beta_1^{-1} & 0 \\ 0 & \beta_1 \end{pmatrix} , \quad \mathcal{B}_{1R} = \begin{pmatrix} \beta_1 & 0 \\ 0 & \beta_1^{-1} \end{pmatrix} , \quad (10)$$

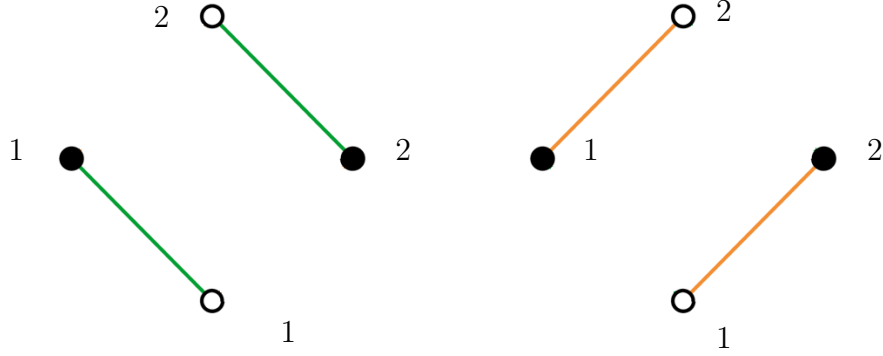


Figure 10: The β -parameter assignments to diamond edges.

while, for the yellow lines, the associated matrices are

$$\mathcal{B}_{2L} = \begin{pmatrix} 0 & \beta_2 \\ \beta_2^{-1} & 0 \end{pmatrix} \quad , \quad \mathcal{B}_{2R} = \begin{pmatrix} 0 & \beta_2 \\ \beta_2^{-1} & 0 \end{pmatrix} \quad . \quad (11)$$

Multiplying $\mathcal{B}_{1R}\mathcal{B}_{2L}$ together with the vector of fermions, Ψ , is equivalent to an automorphism along the yellow, and then green lines from one fermion node to the other. To make this path tracing more explicit, let us first define the color dependent block matrix, which permutes the super vector $\Phi \oplus \Psi$ as defined below.

Definition 1 :

Let the matrix \mathbf{C}_j be the color block matrix associated with the J^{th} line color. We define

$$\mathbf{C}_j \equiv \begin{pmatrix} 0 & \mathcal{B}_{jR} \\ \mathcal{B}_{jL} & 0 \end{pmatrix} \quad , \quad (12)$$

to represent the permutation on the vector of bosons and fermions by the operator D_j . Thus, when we trace a path from one node to another via the green line, we are really multiplying the vector of fermions and bosons, $\Phi \oplus \Psi$ by \mathbf{C}_1 .

Therefore, multiplying the matrices $\mathbf{C}_1\mathbf{C}_2$ for the bow For the bow tie in Fig. # 8, we find that

$$\mathbf{C}_1\mathbf{C}_2 = \begin{pmatrix} 0 & \beta_2^{-1}\beta_1 & 0 & 0 \\ \beta_2^{-1}\beta_1 & 0 & 0 & 0 \\ 0 & 0 & 0 & \beta_2\beta_1^{-1} \\ 0 & 0 & \beta_2\beta_1^{-1} & 0 \end{pmatrix} \quad , \quad (13)$$

in comparison, the diamond 2-color path in Fig. # 8 yields

$$\mathbf{C}_1\mathbf{C}_2 = \begin{pmatrix} 0 & \beta_2\beta_1 & 0 & 0 \\ \beta_2^{-1}\beta_1^{-1} & 0 & 0 & 0 \\ 0 & 0 & 0 & \beta_2^{-1}\beta_1 \\ 0 & 0 & \beta_2\beta_1^{-1} & 0 \end{pmatrix} . \quad (14)$$

tie traces part of the bow tie path starting from every node. Because it is the relative position of nodes along a path that distinguishes diamonds and bow ties, we will show that examining the C_1C_2 block matrix will tell us which 2-color loop is which. The difference between these two 2-color paths becomes apparent by studying the matrix eigenvalues. The eigenvalues of the color block matrix are $\pm\{\beta_2\beta_1^{-1}, \beta_2^{-1}\beta_1\}$, while the diamond adinkra's eigenvalues are ± 1 . We don't even have to find the eigenvalues of the entire matrix, however because the upper matrix $\mathcal{B}_{IL}\mathcal{B}_{JR}$ already says the number of bow ties. Intuitively, we can see this by remembering that the non-zero elements in $\mathcal{B}_{IL}\mathcal{B}_{JR}$ record the path along half of a 2-color loop for each boson (as there are two bosons in each 2-color loop, the relative positions of nodes in the entire loop is recorded). The eigenvalues record the relative positions of the lines as we move around the full 2-color loop. Thus, if we move around a diamond adinkra, we move down lines of color I and J and then back up another pair of lines of color I and J on our return trip. Recording the round trip gives us the values

$$\pm\beta_I\beta_J\beta_I^{-1}\beta_J^{-1} = \pm 1 \quad . \quad (15)$$

Similarly, a bow tie 2-color loop's possible eigenvalues are

$$\pm\beta_I^{-1}\beta_J, \quad \pm\beta_I\beta_J^{-1} \quad . \quad (16)$$

Let us define a set S of line colors I such that I and J create bow ties for some $J \in S$ (if no bow ties exist for the color I, then then $S = J$). Then we can say an ambidextrous adinkra is liftable if and only if $\exists S'$ of line colors $I' \notin S$ such that I' and J' create bow ties for some $J' \in S'$ (where similarly if J' doesn't exist, $S'=I'$): $\forall I \in S$ and $I' \in S'$,

$$\text{evals} [\mathcal{B}_{IR}\mathcal{B}_{I'L}] = \pm 1 \quad . \quad (17)$$

In other words, there exists at least two sets of line colors which don't create bow ties with each other.

5 Emergence of the Lorentzian World Sheet

There is one aspect of this approach that likely needs to be explained in further detail: how does an extra dimension appear simply by adding the helicity to the one

dimensional spinors? This part of the story begins with the algebra of the D's and their realization on valise supermultiplets. By definition, the 'L-matrices' satisfy the conditions,

$$\begin{aligned} (L_I)_{i\hat{j}} (R_J)_{\hat{j}}^k + (L_J)_{i\hat{j}} (R_I)_{\hat{j}}^k &= 2 \delta_{IJ} \delta_i^k , \\ (R_J)_{i\hat{j}} (L_I)_{\hat{j}}^{\hat{k}} + (R_I)_{i\hat{j}} (L_J)_{\hat{j}}^{\hat{k}} &= 2 \delta_{IJ} \delta_i^{\hat{k}} , \end{aligned} \quad (18)$$

where

$$(R_I)_{\hat{j}}^k \delta_{ik} = (L_I)_i^{\hat{k}} \delta_{j\hat{k}} . \quad (19)$$

For a fixed size d , there are $2^{d-1}d!$ distinct matrices that can be used. Given a set of such L-matrices, one can introduce d bosons Φ_i ($i = 1, \dots, d$) and d fermions $\Psi_{\hat{k}}$ ($\hat{k} = 1, \dots, d$) along with N superderivatives D_I ($I = 1, \dots, N$) that satisfy the equations

$$D_I \Phi_i = i (L_I)_{i\hat{k}} \Psi_{\hat{k}} , \quad D_I \Psi_{\hat{k}} = (R_I)_{\hat{k}i} \partial_\tau \Phi_i . \quad (20)$$

The definitions in (18), (19), and (20) will ensure that these $D = 1$ bosons and fermions form a representation of N -extended SUSY. It is a requirement of the construction that both Φ_i and $\Psi_{\hat{k}}$ are functions of a single time-like parameter τ . These equations ensure that the operator equation

$$D_I D_J + D_J D_I = i 2 \delta_{IJ} \partial_\tau , \quad (21)$$

is satisfied on all bosons and fermions.

When a plus or minus helicity index is appended to the D-operator in the first equation in (20) that index must consistently appear on both sides.

$$D_I \Phi_i = i (L_I)_{i\hat{k}} \Psi_{\hat{k}} \rightarrow D_{\pm I} \Phi_i = i (L_I)_{i\hat{k}} \Psi_{\pm \hat{k}} . \quad (22)$$

So the helicity assignment to the D-operators implies a helicity assignment to the spinors. Note there is not any requirement that the same helicity assignment be made for all the spinors. Some can have plus signs while other may have minus signs. The choice of which numerical values of the spinorial index corresponds to plus and which to minus is the information carried by the operator $\text{Spin}(D_I)$ and we have

$$\text{Spin}(D_I) \Phi_i = i (L_I)_{i\hat{k}} \text{Spin}(\Psi_{\hat{k}}) , \quad (23)$$

since the bosons are all assumed to be scalars.

Now we can consider the effect of the appended helicity assignments on the equation in (21) so that it becomes

$$\text{Spin}(D_I) \text{Spin}(D_J) + \text{Spin}(D_J) \text{Spin}(D_I) = i 2 \delta_{IJ} \text{Spin}(\partial_\tau) . \quad (24)$$

If the spin assignments of both D_I and D_J are positive, then we can assign twice these individual helicities to $\text{Spin}(\partial_\tau)$ and call the new derivative ∂_+ . As the subscript on this new operator indicates, its helicity is the same as two plus signs and we ‘stack’ these two signs one on top of the other in a space saving manner. If the spin assignments of both D_I and D_J are negative, then we can assign twice these individual helicities to $\text{Spin}(\partial_\tau)$ and call the new derivative ∂_- . Once more as the subscript on this new operator indicates, its helicity is the same as two minus signs and we ‘stack’ these two signs one on top of the other in a space saving manner. If the spin assignment of D_I is different from that of D_J it is consistent to set the RHS of (24) to zero. So in the presence of helicity assignments to the D-operators we have

$$\begin{aligned} \text{Spin}(D_I)\text{Spin}(D_J) + \text{Spin}(D_J)\text{Spin}(D_I) &= i2 \delta_{IJ} \partial_+ \quad ; \text{if } \text{Spin}(D_I) = \text{Spin}(D_J) = \frac{1}{2} \\ \text{Spin}(D_I)\text{Spin}(D_J) + \text{Spin}(D_J)\text{Spin}(D_I) &= i2 \delta_{IJ} \partial_- \quad ; \text{if } \text{Spin}(D_I) = \text{Spin}(D_J) = -\frac{1}{2} \\ \text{Spin}(D_I)\text{Spin}(D_J) + \text{Spin}(D_J)\text{Spin}(D_I) &= 0 \quad ; \text{if } \text{Spin}(D_I) \neq \text{Spin}(D_J) \quad , \end{aligned} \quad (25)$$

in the three respective cases. But there are now *two* distinct bosonic derivative operators ∂_+ and ∂_- . This implies that the functions associated with the nodes can depend on both coordinates conjugate to these two derivatives. In the case of the diamond (which corresponds to the case of the $d = 2$ and $N = 2$ valise but with one node lifted), we see

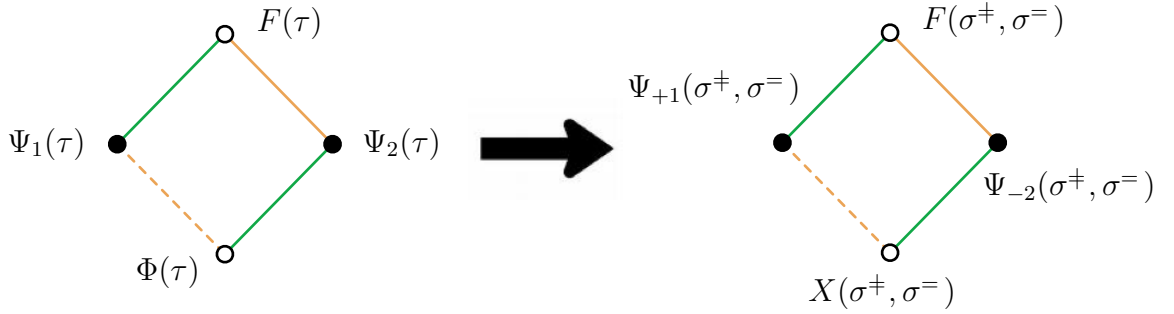


Figure 11: Addition of helicity and two dimensions emergence.

which shows the effect of adding the ambidextrous helicity. Thus, the diamond adinkra in 1D gives rise to the superfield containing the coordinate $X(\sigma^\pm, \sigma^\pm)$ required to describe the world sheet of the superstring in its RNS formulation.

There is one more bonus to this construction. The two derivatives that appear by this construction are naturally associated with *light-cone* coordinates for a two dimensional manifold with a Lorentzian symmetry.

$$\sigma^\pm = \frac{1}{\sqrt{2}} [\tau + \sigma] \quad , \quad \sigma^\pm = \frac{1}{\sqrt{2}} [\tau - \sigma] \quad . \quad (26)$$

Spin realizing a Lorentzian $(1, 1)$ signature (as compared to a $(2, 0)$ or $(0, 2)$ signature) is certainly *not* an inessential feature of this construction. It is as if adinkras together with helicity conservation, for its own internal consistency, requires a Lorentzian structure and a second coordinate to appear. Thus, the world sheet of superstring theory emerges with remarkable simplicity in this way.

We have thus shown how to start from representations of (21) and derive representations of

$$D_{\alpha i} D_{\beta j} + D_{\beta j} D_{\alpha i} = i 2 \delta_{ij} (\gamma^{\underline{a}})_{\alpha\beta} \partial_{\underline{a}} \quad , \quad (27)$$

i. e., the two dimensional version of supersymmetry with $(\gamma^{\underline{a}})_{\alpha\beta}$ being 2D Dirac matrices and $\partial_{\underline{a}} = (\partial_+, \partial_-)$. Some explicit examples are given in the appendices.

6 Finding the Liftability of the Tesseract & Folded Tesseract Adinkras

In previous works [8], it was shown that four color adinkras have the topology of the tesseract, or by using self-dual block linear error correcting codes, a folded version of the tesseract. Using our algorithm applied to the folded tesseract, we find 6 liftable supermultiplets in Appendix A. The chiral multiplets found agree nicely with Thm. # 1 (where we removed one “non-hypercubic” line to determine liftability). An example of a liftable adinkra is in Fig. # 7. Because the liftable chiral supermultiplets are easy to determine, we used them to test our algorithm on folded adinkras. As we saw in Fig. # 7, all liftable chiral adinkras were determined by removing a single line color, in agreement with Thm. # 1.

In addition, we determined the liftability of tesseract adinkras, as seen in Appendix B (a typical adinkra is seen in Fig. # 6). To determine which adinkras were liftable, we were forced to use Mathematica due to the sheer number of adinkras possible (there were 90 unique adinkras, of which 22 are liftable). We wrote a code that looked at each adinkra, and determined liftability via the above algorithm. Interestingly, the shape of the liftable adinkras make up 5 distinct classes. Almost all adinkras within these classes differ only by placement of line color: some adinkras have red-green bow ties while others have yellow-green bow ties, but all the adinkras within a class “look” the same, ignoring the line color.

As a demonstration of the comprehensive nature of the code and its power to uncover two dimensional supermultiplets it was used on two classes of four color adinkras:

- (a.) adinkras with four black dots and four white dots where the algorithm identified the $(p, q) = (2, 2)$ chiral and twisted chiral $(2|4|2)$ supermultiplets,
- (b.) adinkras with eight black dots and eight white dots where the algorithm identified the following ambidextrous supermultiplets:
 - (1.) the $(p, q) = (2, 2)$ & $(p, q) = (3, 1)$ real scalar $(1|4|6|4|1)$ supermultiplet,
 - (2.) the $(p, q) = (2, 2)$ semi-chiral $(2|6|6|2)$ supermultiplet,
 - (3.) the $(p, q) = (2, 2)$ & $(p, q) = (3, 1)$ $(4|8|4)$ supermultiplets, and
 - (4.) the $(p, q) = (3, 1)$ of $(1|5|7|3)$ and $(3|7|5|1)$ supermultiplets.

Above the notation $(n_1 | n_2 | \dots)$ denotes the number of nodes at each height in the adinkra starting at the bottom, i.e. the fields of lowest engineering dimension.

Before we leave this discussion of liftability, comment seems warranted with regard to a result found in the work of Ref. [5]. The authors analyzed the case of lifting from one dimension the adinkras that correspond to the usual 4D, $\mathcal{N} = 1$ chiral and vector supermultiplets. The adinkras that describe the component fields of a chiral supermultiplet have the form shown for all of the $(2|4|2)$ adinkras in appendix A. The adinkras that describe the component fields of a vector supermultiplet have the $(3|4|1)$ height form.

In our exploration of liftability, we find that the ambidextrous $(3|4|1)$ adinkras *cannot* be lifted to even two dimensions while the $(1|4|6|4|1)$ can be lifted to two dimensions. This is exactly the same as what was found in Ref. [5]. The $(3|4|1)$ adinkra corresponds to a component-level Coulomb and Wess-Zumino gauged-fixed description of the vector supermultiplet. Our current work on dimensional extension to two dimensions and the work in Ref. [5] on dimensional extension to four dimensions both imply that it is the $(1|4|6|4|1)$ adinkra that is liftable in both cases.

As was noted in Ref. [5], this implies that the fields that were zero in the Coulomb and Wess-Zumino gauged-fixed description of a vector supermultiplet must be restored to allow a description compatible with adinkra lifting. Stated in an alternative manner, the component fields of a vector supermultiplet must be embedded into a $(1|4|6|4|1)$ adinkra in order to be lifted. The extra fields were given the name ‘spectators’ in [5] and these precisely correspond to the fields that are zero in a Wess-Zumino and Coulomb gauge.

However, our presentation emphasizes a feature that is obscured by the discussion in Ref. [5]. As we find this condition already emerges in going from one dimension

to two dimensions, this means that the spinor bundles that were introduced in the discussion in Ref. [5] are not critical. It is the absence of two-color ambidextrous bow tie paths that is important.

Furthermore, this is apparently the origin of the gauge symmetries associated with Yang-Mills superfields. The fact that the $(3|4|1)$ exists as a well defined adinkra representation in one dimension but can *only be lifted to two dimensions if it is embedded* into a $(1|4|6|4|1) = (1|4|3|0|0) + (0|0|3|4|1)$ structure implies there must exist some transformations that make the $(1|4|6|4|1)$ adinkra equivalent to the $(3|4|1)$ adinkra. These are precisely the Yang-Mills type gauge transformations acting on the $(1|4|6|4|1)$ adinkra. It is the absence of bow ties that permits gauge superfields to exist in dimensions greater than one.

Our results also show the original of the gauge symmetries associated with the anti-symmetric 2-form is of a similar nature. As shown in the work of [11], there exist a valise formulation of the reduced tensor supermultiplet. Being a valise, it has the height structure of a $(4|4)$ height representation which is actually the Wess-Zumino gauge-fixed and Coulomb gauge-fixed version of a $(4|8|4)$ height representation where the lowest nodes of the $(4|8|4)$ are fermions. This particular $(4|8|4)$ can be decomposed as $(4|8|4) = (4|4|0) + (0|4|4)$. Here, the $(4|4|0)$ is the field strength of the vector multiplet while the $(0|4|4)$ are the components of the tensor supermultiplet that remain in the Wess-Zumino gauge-fixed and Coulomb gauge-fixed version of the tensor supermultiplet. So once again, it is the absence of bow ties that permits gauge superfields to exist in dimensions greater than one.

We thus find the results that of the three distinct adinkras containing four bosonic nodes and four fermionic nodes obtained in [11] to be lifted on a world sheet containing $(p, q) = (2, 2)$ supersymmetry, these must occur as $(2|4|2)$ representations, or contained in $(1|4|6|4|1)$ representations, or within $(4|8|4)$ representations. As the condition of $(p, q) = (2, 2)$ supersymmetry is a precursor for a full 4D, $\mathcal{N} = 1$ theory, these are precisely the configurations needed to obtain the full 4D, $\mathcal{N} = 1$ chiral, vector, and tensor supermultiplets respectively.

7 Conclusions

It has been our position [4], that traditional and by now standard approaches to understanding the representation theory of off-shell supersymmetry in *all* dimensions beyond one leave enormous room for additional development. This was the primary reason in 2001 we launched a program to tackle such problems. The results of this

search have been the discovery of previously unknown connections to mathematical structures that have been hidden by the traditional approaches to supersymmetrical theories.

However, the greatest benefits to possessing a clean and concise understanding of the mathematical origins of supersymmetrical representation theory go beyond the purely theoretical and academic understanding of the subject. There are practical benefits to be obtained.

The first such benefit for higher dimensional supersymmetry multiplets occurred in the work of Ref. [10]. In this past work, a new off-shell representation of 4D, $\mathcal{N} = 2$ supersymmetry was presented. Though much more study on this must be done, it is possible this will give new insight into the off-shell structure of the standard $\mathcal{N} = 2$ hypermultiplet. Although the methods used to present this supermultiplet were not manifestly based on adinkras, it was adinkra-based concepts utilized by one of the authors of the work that gave an *a priori* indication that such a higher dimensional supermultiplet existed.

In the current presentation, included in the appendices, we give evidence for the discovery of a new 2D, $\mathcal{N} = 2$ supermultiplet with 8 - 8 components. Should this interpretation receive wider validation, it will provide further vindication for initiating this approach to understanding off-shell supersymmetrical representation theory and show the benefits of being able to systematically scan the zoo of 1D adinkras to find those that are liftable to 2D. Let us also note that this new representation is the Klein flipped version of the chiral spinor superfield reduced to two dimensions. Once more as this is not a representation that has been discussed previously, we see the utility of a systematic search of the adinkra zoo.

We have shown that the state-of-the-art in the program has come to the point where an algorithm can be written to search for two dimensional off-shell supermultiplets. Our scan of the 1D adinkra zoo has been limited, but there are no *a priori* reasons it could not be extended to a broader search for more two dimensional supersymmetric representations. We know of no other approaches that efficiently and practically allow for such a search to be undertaken.

Added Note In Proof After the completion of this work, we were reminded of the research by James Park [12] which also explores the liftability of bowtie and diamond adinkras, but utilizing the compatibility conditions described in the work in [5].

“The soul never thinks without a picture. ”

– Aristotle

Acknowledgments

This research was supported in part by the endowment of the John S. Toll Professorship, the University of Maryland Center for String & Particle Theory, National Science Foundation Grant PHY-09-68854. KB would like to thank Thomas Rimlinger for determining liftable adinkras by hand, in order to check over the Mathematica code. Additionally KB acknowledges participation in 2012 SSTPRS (Student Summer Theoretical Physics Research Session). Adinkras were drawn with *Adinkramat* © 2008 by G. Landweber.

Appendix A: Lifiable 2D Folded-Tesseract Based Adinkras & Associated 2D SUSY Equations

Here we present liftable $(2|4|2)$ ambidextrous supermultiplet adinkras and associated 2D SUSY equations. Below are the liftable adinkras.

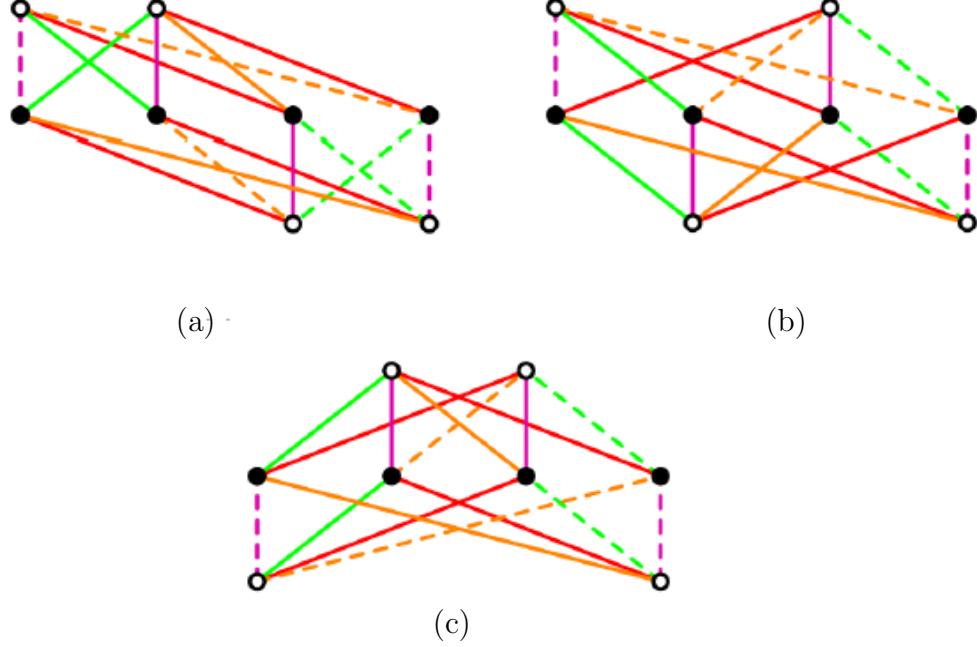


Figure 12: The liftable $(2|4|2)$ folded-tesseract based adinkras

Let us define green, orange, red and purple line colors to be associated with the the subscripts “1”, “2”, “3”, and “4”, respectively. We label open (boson) nodes as Φ_i , where the “ i ” subscript lexicographically labels nodes along each row from left to right, where the top left open node is Φ_1 . Closed nodes corresponding to fermion fields are labeled $\Psi_{\hat{k}}$, where the “ \hat{k} ” subscript is organized analogously. The SUSY equations for (a) are:

$$\begin{aligned}
 D_{1-}\Phi_1 &= i\partial_{=}\Psi_{2+} , & D_{2+}\Phi_1 &= -i\partial_{\neq}\Psi_{4-} , & D_{3+}\Phi_1 &= i\partial_{\neq}\Psi_{3-} , & D_{4-}\Phi_1 &= -i\partial_{=}\Psi_{1+} , \\
 D_{1-}\Phi_2 &= i\partial_{=}\Psi_{1+} , & D_{2+}\Phi_2 &= i\partial_{\neq}\Psi_{3-} , & D_{3+}\Phi_2 &= i\partial_{\neq}\Psi_{4-} , & D_{4-}\Phi_2 &= i\partial_{=}\Psi_{2+} , \\
 D_{1-}\Phi_3 &= -i\Psi_{4-} , & D_{2+}\Phi_3 &= -i\Psi_{2+} , & D_{3+}\Phi_3 &= i\Psi_{1+} , & D_{4-}\Phi_3 &= i\Psi_{3-} , \\
 D_{1-}\Phi_4 &= -i\Psi_{3-} , & D_{2+}\Phi_4 &= i\Psi_{1+} , & D_{3+}\Phi_4 &= i\Psi_{2+} , & D_{4-}\Phi_4 &= -i\Psi_{4-} , \\
 D_{1-}\Psi_{1+} &= \Phi_2 , & D_{2+}\Psi_{1+} &= \partial_{\neq}\Phi_4 , & D_{3+}\Psi_{1+} &= \partial_{\neq}\Phi_3 , & D_{4-}\Psi_{1+} &= -\Phi_1 , \\
 D_{1-}\Psi_{2+} &= \Phi_1 , & D_{2+}\Psi_{2+} &= -\partial_{\neq}\Phi_3 , & D_{3+}\Psi_{2+} &= \partial_{\neq}\Phi_4 , & D_{4-}\Psi_{2+} &= \Phi_2 , \\
 D_{1-}\Psi_{3-} &= -\partial_{=}\Phi_4 , & D_{2+}\Psi_{3-} &= \Phi_2 , & D_{3+}\Psi_{3-} &= \Phi_1 , & D_{4-}\Psi_{3-} &= \partial_{=}\Phi_3 , \\
 D_{1-}\Psi_{4-} &= -\partial_{=}\Phi_3 , & D_{2+}\Psi_{4-} &= -\Phi_1 , & D_{3+}\Psi_{4-} &= \Phi_2 , & D_{4-}\Psi_{4-} &= -\partial_{=}\Phi_4 .
 \end{aligned}
 \tag{A.1}$$

The SUSY equations for (b) are equivalent with Red $\rightarrow D_1$, Green $\rightarrow D_3$ and Purple $\rightarrow -D_4$. All other colors are defined as they were originally. Similarly, the SUSY equations for (c) are equivalent with Yellow $\rightarrow D_1$, Red $\rightarrow D_2$, and Green $\rightarrow D_3$.

Appendix B: Lifiable 2D Tesseract Based Adinkras & Associated 2D SUSY Equations

In this appendix we present twenty-two liftable ambidextrous adinkras, organized by number of nodes in each row. Below each set, we will present in complete detail a representative of the associated 2D SUSY equations. There are also given a set of redefinition give that allow the construction of the 2D SUSY equations for the other members in each set.

Our initial definitions are such that we define green lines to correspond to the D-operator with the subscript “1”, purple lines to correspond to the D-operator the subscript “2”, red lines to correspond to the D-operator the subscript “3”, and yellow lines to correspond to the D-operator the subscript “4”. We label open (boson) nodes as Φ_i , where the “ i ” subscript lexicographically labels nodes along each row from left to right, where the top left open node is Φ_1 . Closed nodes corresponding to fermion fields are labeled as $\Psi_{\hat{k}}$, where the “ \hat{k} ” subscript is organized analogously. Many adinkras create equivalent equations except with colors re-defined. In this appendix, all colors not explicitly redefined, remain as they were originally defined above.

The first liftable ambidextrous adinkra tesseract-based is shown in Fig. # 13 below.

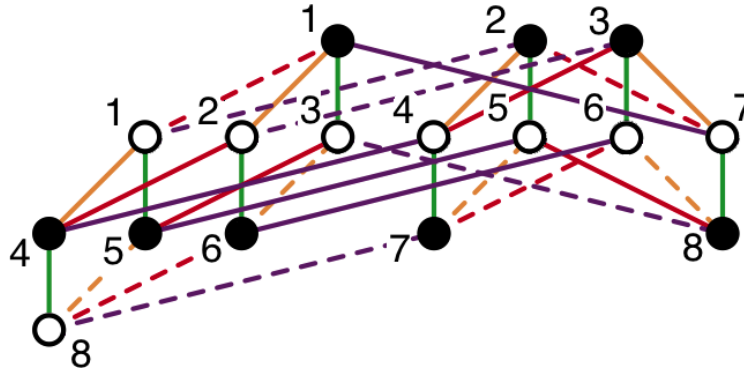


Figure 13: A liftable (1|5|7|3) adinkra with nodal labels shown.

This adinkra may be engineered to produce a $(p, q) = (3, 1)$ superfield. We will use this example to show the nodal labels in the context of the adinkra, although we will not relate field labels to the associated nodes in any of our later demonstrations in

$$\begin{aligned}
D_{1-}\Phi_1 &= i\partial_=\Psi_{5+}, & D_{2+}\Phi_1 &= -i\Psi_{2+}, & D_{3+}\Phi_1 &= -i\Psi_{1+}, & D_{4+}\Phi_1 &= i\partial_+\Psi_{4-}, \\
D_{1-}\Phi_2 &= i\partial_=\Psi_{6+}, & D_{2+}\Phi_2 &= -i\Psi_{3+}, & D_{3+}\Phi_2 &= i\partial_+\Psi_{4-}, & D_{4+}\Phi_2 &= i\Psi_{1+}, \\
D_{1-}\Phi_{3+} &= i\Psi_{1+}, & D_{2+}\Phi_{3+} &= -i\partial_+\Psi_{8+}, & D_{3+}\Phi_{3+} &= i\partial_+\Psi_{5+}, & D_{4+}\Phi_{3+} &= -i\partial_+\Psi_{6+}, \\
D_{1-}\Phi_4 &= i\partial_=\Psi_{7+}, & D_{2+}\Phi_4 &= i\partial_+\Psi_{4-}, & D_{3+}\Phi_4 &= i\Psi_{3+}, & D_{4+}\Phi_4 &= i\Psi_{2+}, \\
D_{1-}\Phi_{5+} &= i\Psi_{2+}, & D_{2+}\Phi_{5+} &= i\partial_+\Psi_{5+}, & D_{3+}\Phi_{5+} &= i\partial_+\Psi_{8+}, & D_{4+}\Phi_{5+} &= -i\partial_+\Psi_{7+}, \\
D_{1-}\Phi_{6+} &= i\Psi_{3+}, & D_{2+}\Phi_{6+} &= i\partial_+\Psi_{6+}, & D_{3+}\Phi_{6+} &= -i\partial_+\Psi_{7+}, & D_{4+}\Phi_{6+} &= -i\partial_+\Psi_{8+}, \\
D_{1-}\Phi_7 &= i\partial_=\Psi_{8+}, & D_{2+}\Phi_7 &= i\Psi_{1+}, & D_{3+}\Phi_7 &= -i\Psi_{2+}, & D_{4+}\Phi_7 &= i\Psi_{3+}, \\
D_{1-}\Phi_8 &= i\Psi_{4-}, & D_{2+}\Phi_8 &= -i\Psi_{7+}, & D_{3+}\Phi_8 &= -i\Psi_{6+}, & D_{4+}\Phi_8 &= -i\Psi_{5+}, \\
D_{1-}\Psi_{1+} &= \partial_=\Phi_{3+}, & D_{2+}\Psi_{1+} &= \partial_+\Phi_7, & D_{3+}\Psi_{1+} &= -\partial_+\Phi_1, & D_{4+}\Psi_{1+} &= \partial_+\Phi_2, \\
D_{1-}\Psi_{2+} &= \partial_=\Phi_{5+}, & D_{2+}\Psi_{2+} &= -\partial_+\Phi_1, & D_{3+}\Psi_{2+} &= -\partial_+\Phi_7, & D_{4+}\Psi_{2+} &= \partial_+\Phi_4, \\
D_{1-}\Psi_{3+} &= \partial_=\Phi_{6+}, & D_{2+}\Psi_{3+} &= -\partial_+\Phi_2, & D_{3+}\Psi_{3+} &= \partial_+\Phi_4, & D_{4+}\Psi_{3+} &= \partial_+\Phi_7, \\
D_{1-}\Psi_{4-} &= \partial_=\Phi_8, & D_{2+}\Psi_{4-} &= \Phi_4, & D_{3+}\Psi_{4-} &= \Phi_2, & D_{4+}\Psi_{4-} &= \Phi_1, \\
D_{1-}\Psi_{5+} &= \Phi_1, & D_{2+}\Psi_{5+} &= \Phi_{5+}, & D_{3+}\Psi_{5+} &= \Phi_{3+}, & D_{4+}\Psi_{5+} &= -\partial_+\Phi_8, \\
D_{1-}\Psi_{6+} &= \Phi_2, & D_{2+}\Psi_{6+} &= \Phi_{6+}, & D_{3+}\Psi_{6+} &= -\partial_+\Phi_8, & D_{4+}\Psi_{6+} &= -\Phi_{3+}, \\
D_{1-}\Psi_{7+} &= \Phi_4, & D_{2+}\Psi_{7+} &= -\partial_+\Phi_8, & D_{3+}\Psi_{7+} &= -\Phi_{6+}, & D_{4+}\Psi_{7+} &= -\Phi_{5+}, \\
D_{1-}\Psi_{8+} &= \Phi_7, & D_{2+}\Psi_{8+} &= -\Phi_{3+}, & D_{3+}\Psi_{8+} &= \Phi_{5+}, & D_{4+}\Psi_{8+} &= -\Phi_{6+},
\end{aligned} \tag{B.1}$$

The bosons have spin 0 (e.g. $\Phi_1, \Phi_2, \Phi_4, \Phi_7, \Phi_8$) or correspond to the positive helicity components of a spin 1 vector (e.g. $\Phi_{3+}, \Phi_{5+}, \Phi_{6+}$). We also note that Ψ_{4-} represents a fermion with spin -1/2 and all other fermions have spin 1/2.

The adinkra shown in Fig. # 14, actually leads to two distinct superfields. One

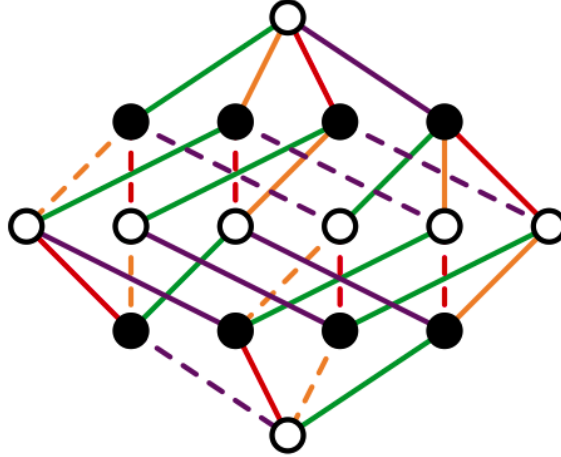


Figure 14: The unique (1|4|6|4|1) fully extended adinkra.

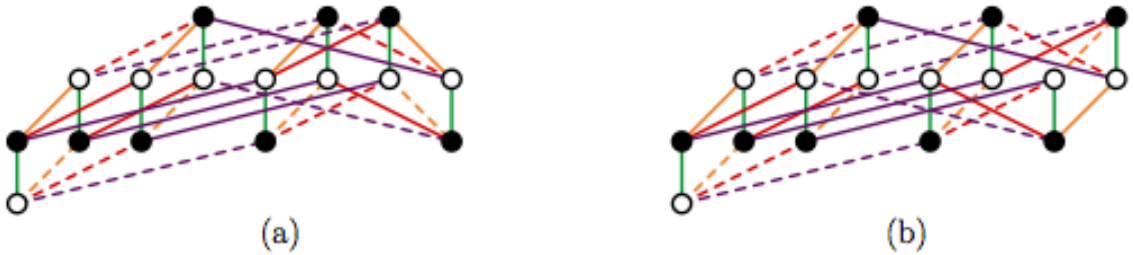
of these corresponds to the dimensional reduction of the well known real scalar su-

perfield from 4D, $\mathcal{N} = 1$ supersymmetry. Accordingly, it has a degree of extended supersymmetry characterized by $(p, q) = (2, 2)$. As this is a familiar representation, we will not discuss it further.

However, there is a second superfield characterized by $(p, q) = (3, 1)$ and as this is the lesser know supersymmetric representation we will concentrate on its structure⁴. The associated 2D SUSY equations (containing a spin 3/2 fermion $\Psi_{8=}$) are:

$$\begin{aligned}
D_{1-}\Phi_1 &= i\partial_{=}\Psi_{1+}, & D_{2+}\Phi_1 &= i\partial_{\neq}\Psi_{4-}, & D_{3+}\Phi_1 &= i\partial_{\neq}\Psi_{3-}, & D_{4+}\Phi_1 &= i\partial_{\neq}\Psi_{2-}, \\
D_{1-}\Phi_2 &= i\Psi_{2-}, & D_{2+}\Phi_2 &= i\partial_{\neq}\Psi_{6-}, & D_{3+}\Phi_2 &= i\partial_{\neq}\Psi_{5-}, & D_{4+}\Phi_2 &= -i\Psi_{1+}, \\
D_{1-}\Phi_3 &= i\Psi_{3-}, & D_{2+}\Phi_3 &= i\partial_{\neq}\Psi_{7-}, & D_{3+}\Phi_3 &= -i\Psi_{1+}, & D_{4+}\Phi_3 &= -i\partial_{\neq}\Psi_{5-}, \\
D_{1-}\Phi_{4=} &= i\partial_{=}\Psi_{5-}, & D_{2+}\Phi_{4=} &= i\partial_{\neq}\Psi_{8=}, & D_{3+}\Phi_{4=} &= -i\Psi_{2-}, & D_{4+}\Phi_{4=} &= i\Psi_{3-}, \\
D_{1-}\Phi_5 &= i\Psi_{4-}, & D_{2+}\Phi_5 &= -i\Psi_{1+}, & D_{3+}\Phi_5 &= -i\partial_{\neq}\Psi_{7-}, & D_{4+}\Phi_5 &= -i\partial_{\neq}\Psi_{6-}, \\
D_{1-}\Phi_{6=} &= i\partial_{=}\Psi_{6-}, & D_{2+}\Phi_{6=} &= -i\Psi_{2-}, & D_{3+}\Phi_{6=} &= -i\partial_{\neq}\Psi_{8=}, & D_{4+}\Phi_{6=} &= i\Psi_{4-}, \\
D_{1-}\Phi_{7=} &= i\partial_{=}\Psi_{7-}, & D_{2+}\Phi_{7=} &= -i\Psi_{3-}, & D_{3+}\Phi_{7=} &= i\Psi_{4-}, & D_{4+}\Phi_{7=} &= i\partial_{\neq}\Psi_{8=}, \\
D_{1-}\Phi_{8=} &= i\Psi_{8=}, & D_{2+}\Phi_{8=} &= -i\Psi_{5-}, & D_{3+}\Phi_{8=} &= i\Psi_{6-}, & D_{4+}\Phi_{8=} &= -i\Psi_{7-}, \\
D_{1-}\Psi_{1+} &= \Phi_1, & D_{2+}\Psi_{1+} &= -\partial_{\neq}\Phi_5, & D_{3+}\Psi_{1+} &= -\partial_{\neq}\Phi_3, & D_{4+}\Psi_{1+} &= -\partial_{\neq}\Phi_2, \\
D_{1-}\Psi_{2-} &= \partial_{=}\Phi_2, & D_{2+}\Psi_{2-} &= -\partial_{\neq}\Phi_{6=}, & D_{3+}\Psi_{2-} &= -\partial_{\neq}\Phi_{4=}, & D_{4+}\Psi_{2-} &= \Phi_1, \\
D_{1-}\Psi_{3-} &= \partial_{=}\Phi_3, & D_{2+}\Psi_{3-} &= -\partial_{\neq}\Phi_{7=}, & D_{3+}\Psi_{3-} &= \Phi_1, & D_{4+}\Psi_{3-} &= \partial_{\neq}\Phi_{4=}, \\
D_{1-}\Psi_{4-} &= \partial_{=}\Phi_5, & D_{2+}\Psi_{4-} &= \Phi_1, & D_{3+}\Psi_{4-} &= \partial_{\neq}\Phi_{7=}, & D_{4+}\Psi_{4-} &= \partial_{\neq}\Phi_{6=}, \\
D_{1-}\Psi_{5-} &= \Phi_{4=}, & D_{2+}\Psi_{5-} &= -\partial_{\neq}\Phi_{8=}, & D_{3+}\Psi_{5-} &= \Phi_2, & D_{4+}\Psi_{5-} &= -\Phi_3, \\
D_{1-}\Psi_{6-} &= \Phi_{6=}, & D_{2+}\Psi_{6-} &= \Phi_2, & D_{3+}\Psi_{6-} &= \partial_{\neq}\Phi_{8=}, & D_{4+}\Psi_{6-} &= -\Phi_5, \\
D_{1-}\Psi_{7-} &= \Phi_{7=}, & D_{2+}\Psi_{7-} &= \Phi_3, & D_{3+}\Psi_{7-} &= -\Phi_5, & D_{4+}\Psi_{7-} &= -\partial_{\neq}\Phi_{8=}, \\
D_{1-}\Psi_{8=} &= \partial_{=}\Phi_{8=}, & D_{2+}\Psi_{8=} &= \Phi_{4=}, & D_{3+}\Psi_{8=} &= -\Phi_{6=}, & D_{4+}\Psi_{8=} &= \Phi_{7=}.
\end{aligned} \tag{B.2}$$

For the next set of four graphs shown in Fig. # 15 and for which we will explicitly present a representative set of equations correspond to:



⁴Of course there is also the possibility of $(p, q) = (1, 3)$ but this is simply the parity reflection of the $(p, q) = (3, 1)$ superfield.

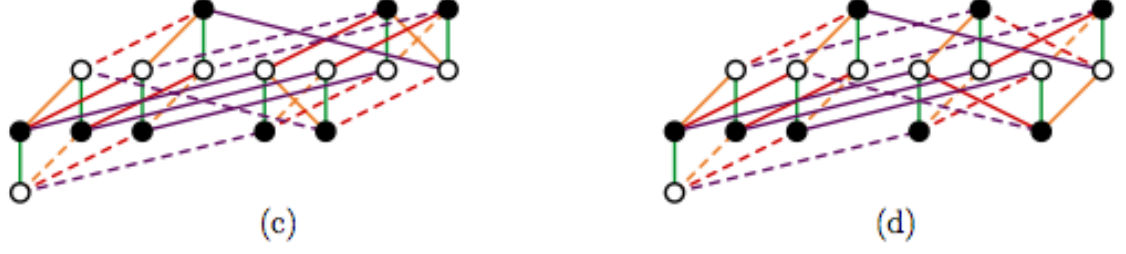


Figure 15: All adinkras of the form (1|5|7|3) that lift to two dimensions.

For Fig. # 14(a), the associated SUSY equations are:

$$\begin{aligned}
D_{1-}\Phi_1 &= i\partial_=\Psi_{5+}, & D_{2+}\Phi_1 &= -i\Psi_{2+}, & D_{3+}\Phi_1 &= -i\Psi_{1+}, & D_{4+}\Phi_1 &= i\partial_+\Psi_{4-}, \\
D_{1-}\Phi_2 &= i\partial_=\Psi_{6+}, & D_{2+}\Phi_2 &= -i\Psi_{3+}, & D_{3+}\Phi_2 &= i\partial_+\Psi_{4-}, & D_{4+}\Phi_2 &= i\Psi_{1+}, \\
D_{1-}\Phi_{3+} &= i\Psi_{1+}, & D_{2+}\Phi_{3+} &= -i\partial_+\Psi_{8+}, & D_{3+}\Phi_{3+} &= i\partial_+\Psi_{5+}, & D_{4+}\Phi_{3+} &= -i\partial_+\Psi_{6+}, \\
D_{1-}\Phi_4 &= i\partial_=\Psi_{7+}, & D_{2+}\Phi_4 &= i\partial_+\Psi_{4-}, & D_{3+}\Phi_4 &= i\Psi_{3+}, & D_{4+}\Phi_4 &= i\Psi_{2+}, \\
D_{1-}\Phi_{5+} &= i\Psi_{2+}, & D_{2+}\Phi_{5+} &= i\partial_+\Psi_{5+}, & D_{3+}\Phi_{5+} &= i\partial_+\Psi_{8+}, & D_{4+}\Phi_{5+} &= -i\partial_+\Psi_{7+}, \\
D_{1-}\Phi_{6+} &= i\Psi_{3+}, & D_{2+}\Phi_{6+} &= i\partial_+\Psi_{6+}, & D_{3+}\Phi_{6+} &= -i\partial_+\Psi_{7+}, & D_{4+}\Phi_{6+} &= -i\partial_+\Psi_{8+}, \\
D_{1-}\Phi_7 &= i\partial_=\Psi_{8+}, & D_{2+}\Phi_7 &= i\Psi_{1+}, & D_{3+}\Phi_7 &= -i\Psi_{2+}, & D_{4+}\Phi_7 &= i\Psi_{3+}, \\
D_{1-}\Phi_8 &= i\Psi_{4-}, & D_{2+}\Phi_8 &= -i\Psi_{7+}, & D_{3+}\Phi_8 &= -i\Psi_{6+}, & D_{4+}\Phi_8 &= -i\Psi_{5+}, \\
D_{1-}\Psi_{1+} &= \partial_=\Phi_{3+}, & D_{2+}\Psi_{1+} &= \partial_+\Phi_7, & D_{3+}\Psi_{1+} &= -\partial_+\Phi_1, & D_{4+}\Psi_{1+} &= \partial_+\Phi_2, \\
D_{1-}\Psi_{2+} &= \partial_=\Phi_{5+}, & D_{2+}\Psi_{2+} &= -\partial_+\Phi_1, & D_{3+}\Psi_{2+} &= -\partial_+\Phi_7, & D_{4+}\Psi_{2+} &= \partial_+\Phi_4, \\
D_{1-}\Psi_{3+} &= \partial_=\Phi_{6+}, & D_{2+}\Psi_{3+} &= -\partial_+\Phi_2, & D_{3+}\Psi_{3+} &= \partial_+\Phi_4, & D_{4+}\Psi_{3+} &= \partial_+\Phi_7, \\
D_{1-}\Psi_{4-} &= \partial_=\Phi_8, & D_{2+}\Psi_{4-} &= \Phi_4, & D_{3+}\Psi_{4-} &= \Phi_2, & D_{4+}\Psi_{4-} &= \Phi_1, \\
D_{1-}\Psi_{5+} &= \Phi_1, & D_{2+}\Psi_{5+} &= \Phi_{5+}, & D_{3+}\Psi_{5+} &= \Phi_{3+}, & D_{4+}\Psi_{5+} &= -\partial_+\Phi_8, \\
D_{1-}\Psi_{6+} &= \Phi_2, & D_{2+}\Psi_{6+} &= \Phi_{6+}, & D_{3+}\Psi_{6+} &= -\partial_+\Phi_8, & D_{4+}\Psi_{6+} &= -\Phi_{3+}, \\
D_{1-}\Psi_{7+} &= \Phi_4, & D_{2+}\Psi_{7+} &= -\partial_+\Phi_8, & D_{3+}\Psi_{7+} &= -\Phi_{6+}, & D_{4+}\Psi_{7+} &= -\Phi_{5+}, \\
D_{1-}\Psi_{8+} &= \Phi_7, & D_{2+}\Psi_{8+} &= -\Phi_{3+}, & D_{3+}\Psi_{8+} &= \Phi_{5+}, & D_{4+}\Psi_{8+} &= -\Phi_{6+}.
\end{aligned} \tag{B.3}$$

The other adinkras have equivalent equations with color redefinitions. To create the corresponding SUSY equations for the other adinkras in Fig. # 14, we first redefine colors according to:

(b). Green $\rightarrow D_4$	(c.) Green $\rightarrow D_4$	(d.) Green $\rightarrow D_3$
Yellow $\rightarrow D_1$	Yellow $\rightarrow D_3$	Yellow $\rightarrow D_4$
	Red $\rightarrow D_1$	Red $\rightarrow D_2$
		Purple $\rightarrow D_1$

So that we see the need to redefine only two colors in case (b), three in case (c) and all four in case (d). The corresponding equations are not the exact same, however, due to differences in line dashing. We may, however, re-create the exact same equations with node redefinitions, (e.g. $\Phi_i \rightarrow -\Phi_i$) in the cases of (b) and (d). We do note, however, if one set of equation has an odd number of line dashing relative to another, the two sets of equation describe a supermultiplet and its twisted version[11].

Turning to the adinkras in Fig. # 16 shown below. We find six cases of adinkras that can lifted. They can be used to engineer $(p, q) = (2, 2)$ semi-chiral superfields [13], [14], and [15].

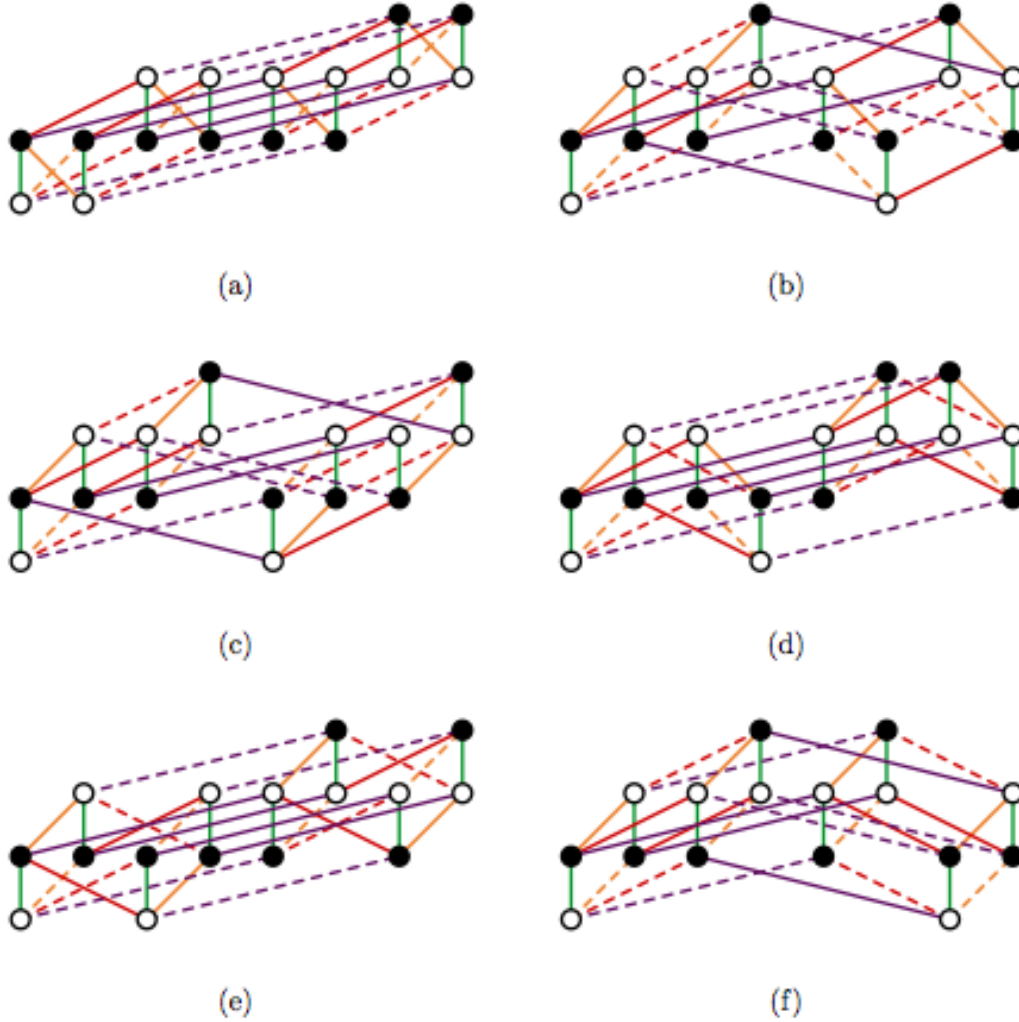


Figure 16: All adinkras of the form $(2|6|6|2)$ that lift to two dimensions. The associated equations for the adinkra in Fig. # 16(a) are:

$$\begin{aligned} D_{1-}\Phi_1 &= i\partial_{=}\Psi_{5+}, & D_{2+}\Phi_1 &= -i\Psi_{1+}, & D_{3+}\Phi_1 &= i\partial_{\neq}\Psi_{3-}, & D_{4-}\Phi_1 &= i\partial_{\neq}\Psi_{6-}, \\ D_{1-}\Phi_2 &= i\partial_{=}\Psi_{6+}, & D_{2+}\Phi_2 &= -i\Psi_{2+}, & D_{3+}\Phi_2 &= i\partial_{\neq}\Psi_{4-}, & D_{4-}\Phi_2 &= -i\partial_{=}\Psi_{5+}, \end{aligned}$$

$$\begin{aligned}
D_{1-}\Phi_3 &= i\partial_{=}\Psi_{7+}, & D_{2+}\Phi_3 &= i\partial_{\neq}\Psi_{3-}, & D_{3+}\Phi_3 &= i\Psi_{1+}, & D_{4-}\Phi_3 &= i\partial_{=}\Psi_{8+}, \\
D_{1-}\Phi_4 &= i\partial_{=}\Psi_{8+}, & D_{2+}\Phi_4 &= i\partial_{\neq}\Psi_{4-}, & D_{3+}\Phi_4 &= i\Psi_{2+}, & D_{4-}\Phi_4 &= -i\partial_{=}\Psi_{7+}, \\
D_{1-}\Phi_{5\neq} &= i\Psi_{1+}, & D_{2+}\Phi_{5\neq} &= i\partial_{\neq}\Psi_{5+}, & D_{3+}\Phi_{5\neq} &= -i\partial_{\neq}\Psi_{7+}, & D_{4-}\Phi_{5\neq} &= -i\Psi_{2+}, \\
D_{1-}\Phi_{6\neq} &= i\Psi_{2+}, & D_{2+}\Phi_{6\neq} &= i\partial_{\neq}\Psi_{6+}, & D_{3+}\Phi_{6\neq} &= -i\partial_{\neq}\Psi_{8+}, & D_{4-}\Phi_{6\neq} &= i\Psi_{1+}, \\
D_{1-}\Phi_7 &= i\Psi_{3-}, & D_{2+}\Phi_7 &= -i\Psi_{7+}, & D_{3+}\Phi_7 &= -i\Psi_{5+}, & D_{4-}\Phi_7 &= -i\Psi_{4-}, \\
D_{1-}\Phi_8 &= i\Psi_{4-}, & D_{2+}\Phi_8 &= -i\Psi_{8+}, & D_{3+}\Phi_8 &= -i\Psi_{6+}, & D_{4-}\Phi_8 &= i\Psi_{3-}, \\
D_{1-}\Psi_{1+} &= \partial_{=}\Phi_{5\neq}, & D_{2+}\Psi_{1+} &= -\partial_{\neq}\Phi_1, & D_{3+}\Psi_{1+} &= \partial_{\neq}\Phi_3, & D_{4-}\Psi_{1+} &= \partial_{=}\Phi_{6\neq}, \\
D_{1-}\Psi_{2+} &= \partial_{=}\Phi_{6\neq}, & D_{2+}\Psi_{2+} &= -\partial_{\neq}\Phi_2, & D_{3+}\Psi_{2+} &= \partial_{\neq}\Phi_4, & D_{4-}\Psi_{2+} &= -\partial_{=}\Phi_{5\neq}, \\
D_{1-}\Psi_{3-} &= \partial_{=}\Phi_7, & D_{2+}\Psi_{3-} &= \Phi_3, & D_{3+}\Psi_{3-} &= \Phi_1, & D_{4-}\Psi_{3-} &= \partial_{=}\Phi_8, \\
D_{1-}\Psi_{4-} &= \partial_{=}\Phi_8, & D_{2+}\Psi_{4-} &= \Phi_4, & D_{3+}\Psi_{4-} &= \Phi_2, & D_{4-}\Psi_{4-} &= -\partial_{=}\Phi_7, \\
D_{1-}\Psi_{5+} &= \Phi_1, & D_{2+}\Psi_{5+} &= \Phi_{5\neq}, & D_{3+}\Psi_{5+} &= -\partial_{\neq}\Phi_7, & D_{4-}\Psi_{5+} &= -\Phi_2, \\
D_{1-}\Psi_{6+} &= \Phi_2, & D_{2+}\Psi_{6+} &= \Phi_{6\neq}, & D_{3+}\Psi_{6+} &= -\partial_{\neq}\Phi_8, & D_{4-}\Psi_{6+} &= \Phi_1, \\
D_{1-}\Psi_{7+} &= \Phi_3, & D_{2+}\Psi_{7+} &= -\partial_{\neq}\Phi_7, & D_{3+}\Psi_{7+} &= -\Phi_{5\neq}, & D_{4-}\Psi_{7+} &= -\Phi_4, \\
D_{1-}\Psi_{8+} &= \Phi_4, & D_{2+}\Psi_{8+} &= -\partial_{\neq}\Phi_8, & D_{3+}\Psi_{8+} &= -\Phi_{6\neq}, & D_{4-}\Psi_{8+} &= \Phi_3.
\end{aligned}
\tag{B.4}$$

To create equivalent equations for the other adinkras in Fig. # 16 from those in Fig. # 16 (a), we re-defining the colors as follows:

(b.) Green $\rightarrow D_1$	(c.) Green $\rightarrow D_3$	(d.) Green $\rightarrow D_1$
Yellow $\rightarrow D_3$	Yellow $\rightarrow D_4$	Yellow $\rightarrow D_2$
Red $\rightarrow D_4$	Red $\rightarrow D_1$	Red $\rightarrow D_3$
		Purple $\rightarrow D_4$
(e.) Green $\rightarrow D_3$	(f.) Green $\rightarrow D_2$	
Yellow $\rightarrow D_1$	Yellow $\rightarrow D_3$	
Red $\rightarrow D_2$	Red $\rightarrow D_4$	
Purple $\rightarrow D_4$	Purple $\rightarrow D_1$	

The graphs in Fig. # 17 below provide adinkras as a basis to engineer $(p, q) = (3, 1)$ supermultiplets. The associated equations from adinkra in Fig. # 16(a) are:

$$\begin{aligned}
D_{1-}\Phi_1 &= i\partial_{=}\Psi_{2+}, & D_{2+}\Phi_1 &= -i\partial_{\neq}\Psi_{6-}, & D_{3+}\Phi_1 &= -i\partial_{\neq}\Psi_{4-}, & D_{4+}\Phi_1 &= -i\partial_{\neq}\Psi_{3-}, \\
D_{1-}\Phi_2 &= i\partial_{=}\Psi_{5+}, & D_{2+}\Phi_2 &= -i\Psi_{1+}, & D_{3+}\Phi_2 &= i\partial_{\neq}\Psi_{3-}, & D_{4+}\Phi_2 &= -i\partial_{\neq}\Psi_{4-}, \\
D_{1-}\Phi_3 &= i\partial_{=}\Psi_{7+}, & D_{2+}\Phi_3 &= i\partial_{\neq}\Psi_{3-}, & D_{3+}\Phi_3 &= i\Psi_{1+}, & D_{4+}\Phi_3 &= -i\partial_{\neq}\Psi_{6-}, \\
D_{1-}\Phi_4 &= i\partial_{=}\Psi_{8+}, & D_{2+}\Phi_4 &= i\partial_{\neq}\Psi_{4-}, & D_{3+}\Phi_4 &= -i\partial_{\neq}\Psi_{6-}, & D_{4+}\Phi_4 &= -i\Psi_{1+},
\end{aligned}$$

$$\begin{aligned}
D_{1-}\Phi_{5\pm} &= i\Psi_{1+}, & D_{2+}\Phi_{5\pm} &= i\partial_{\pm}\Psi_{5+}, & D_{3+}\Phi_{5\pm} &= -i\partial_{\pm}\Psi_{7+}, & D_{4+}\Phi_{5\pm} &= i\partial_{\pm}\Psi_{8+}, \\
D_{1-}\Phi_6 &= i\Psi_{3-}, & D_{2+}\Phi_6 &= -i\Psi_{7+}, & D_{3+}\Phi_6 &= -i\Psi_{5+}, & D_{4+}\Phi_6 &= i\Psi_{2+}, \\
D_{1-}\Phi_7 &= i\Psi_{4-}, & D_{2+}\Phi_7 &= -i\Psi_{8+}, & D_{3+}\Phi_7 &= i\Psi_{2+}, & D_{4+}\Phi_7 &= i\Psi_{5+}, \\
D_{1-}\Phi_8 &= i\Psi_{6-}, & D_{2+}\Phi_8 &= i\Psi_{2+}, & D_{3+}\Phi_8 &= i\Psi_{8+}, & D_{4+}\Phi_8 &= i\Psi_{7+}, \\
D_{1-}\Psi_{1+} &= \partial_{\pm}\Phi_{5\pm}, & D_{2+}\Psi_{1+} &= -\partial_{\pm}\Phi_2, & D_{3+}\Psi_{1+} &= \partial_{\pm}\Phi_3, & D_{4+}\Psi_{1+} &= -\partial_{\pm}\Phi_4, \\
D_{1-}\Psi_{2+} &= \Phi_1, & D_{2+}\Psi_{2+} &= \partial_{\pm}\Phi_8, & D_{3+}\Psi_{2+} &= \partial_{\pm}\Phi_7, & D_{4+}\Psi_{2+} &= \partial_{\pm}\Phi_6, \\
D_{1-}\Psi_{3-} &= \partial_{\pm}\Phi_6, & D_{2+}\Psi_{3-} &= \Phi_3, & D_{3+}\Psi_{3-} &= \Phi_2, & D_{4+}\Psi_{3-} &= -\Phi_1, \\
D_{1-}\Psi_{4-} &= \partial_{\pm}\Phi_7, & D_{2+}\Psi_{4-} &= \Phi_4, & D_{3+}\Psi_{4-} &= -\Phi_1, & D_{4+}\Psi_{4-} &= -\Phi_2, \\
D_{1-}\Psi_{5+} &= \Phi_2, & D_{2+}\Psi_{5+} &= \Phi_{5\pm}, & D_{3+}\Psi_{5+} &= -\partial_{\pm}\Phi_6, & D_{4+}\Psi_{5+} &= \partial_{\pm}\Phi_7, \\
D_{1-}\Psi_{6-} &= \partial_{\pm}\Phi_8, & D_{2+}\Psi_{6-} &= -\Phi_1, & D_{3+}\Psi_{6-} &= -\Phi_4, & D_{4+}\Psi_{6-} &= -\Phi_3, \\
D_{1-}\Psi_{7+} &= \Phi_3, & D_{2+}\Psi_{7+} &= -\partial_{\pm}\Phi_6, & D_{3+}\Psi_{7+} &= -\Phi_{5\pm}, & D_{4+}\Psi_{7+} &= \partial_{\pm}\Phi_8, \\
D_{1-}\Psi_{8+} &= \Phi_4, & D_{2+}\Psi_{8+} &= -\partial_{\pm}\Phi_7, & D_{3+}\Psi_{8+} &= \partial_{\pm}\Phi_8, & D_{4+}\Psi_{8+} &= \Phi_{5\pm}.
\end{aligned} \tag{B.5}$$

To create equivalent equations for the rest of the adinkras in Fig. # 17 from the equations in Fig. # 17(a), we redefine colors below for the other adinkras:

- | | | |
|------------------------------|------------------------------|------------------------------|
| (b). Green $\rightarrow D_4$ | (c.) Green $\rightarrow D_4$ | (d.) Green $\rightarrow D_3$ |
| Yellow $\rightarrow D_1$ | Yellow $\rightarrow D_3$ | Yellow $\rightarrow D_4$ |
| | Red $\rightarrow D_1$ | Red $\rightarrow D_2$ |
| | | Purple $\rightarrow D_1$ |

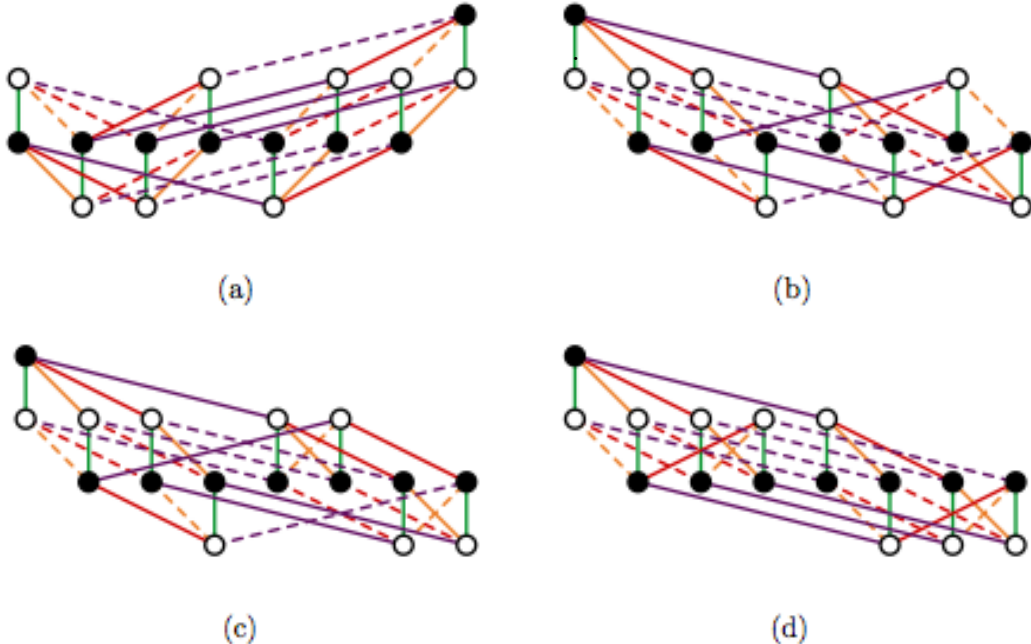


Figure 17: Four (3|7|5|1) adinkras.

There are seven adinkras in our next set of adinkras for engineering. However, they split into two categories: (a)-(d) may be used to create $(p, q) = (3, 1)$ superfields, while (e)-(g) may be used to create $(p, q) = (2, 2)$ superfields. These are all shown in Fig. # 18 below.

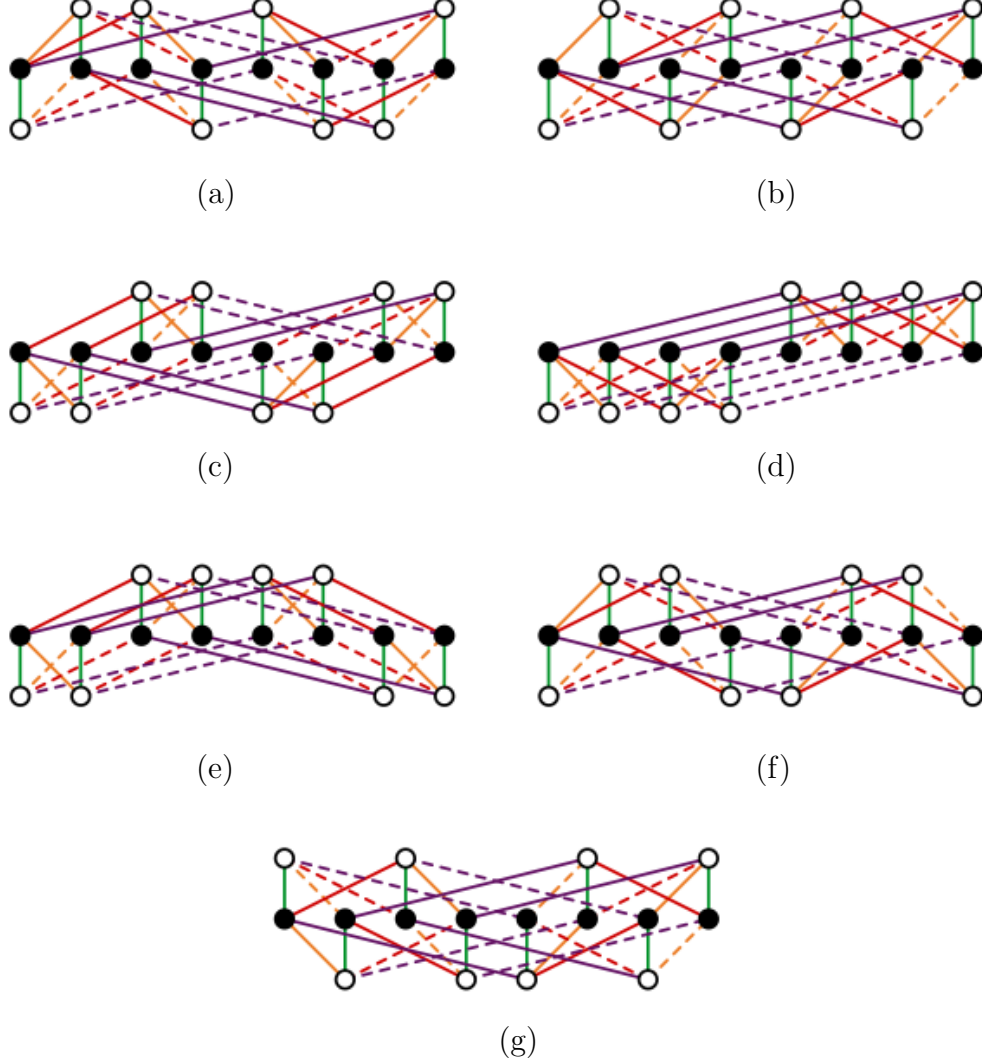


Figure 18: All adinkras of the form $(4|8|4)$ that lift to two dimensions.

The associated equations for the adinkra in Fig # 18(a) are:

$$\begin{aligned}
D_{1-}\Phi_1 &= i\partial_- \Psi_{2+}, & D_{2+}\Phi_1 &= -i\partial_+ \Psi_{6-}, & D_{3+}\Phi_1 &= -i\partial_+ \Psi_{4-}, & D_{4+}\Phi_1 &= i\partial_+ \Psi_{1-}, \\
D_{1-}\Phi_2 &= i\partial_- \Psi_{3+}, & D_{2+}\Phi_2 &= -i\partial_+ \Psi_{7-}, & D_{3+}\Phi_2 &= i\partial_+ \Psi_{1-}, & D_{4+}\Phi_2 &= i\partial_+ \Psi_{4-}, \\
D_{1-}\Phi_3 &= i\partial_- \Psi_{5+}, & D_{2+}\Phi_3 &= i\partial_+ \Psi_{1-}, & D_{3+}\Phi_3 &= i\partial_+ \Psi_{7-}, & D_{4+}\Phi_3 &= i\partial_+ \Psi_{6-}, \\
D_{1-}\Phi_4 &= i\partial_- \Psi_{8+}, & D_{2+}\Phi_4 &= i\partial_+ \Psi_{4-}, & D_{3+}\Phi_4 &= -i\partial_+ \Psi_{6-}, & D_{4+}\Phi_4 &= i\partial_+ \Psi_{7-}, \\
D_{1-}\Phi_5 &= i\Psi_{1-}, & D_{2+}\Phi_5 &= -i\Psi_{5+}, & D_{3+}\Phi_5 &= -i\Psi_{3+}, & D_{4+}\Phi_5 &= -i\Psi_{2+}, \\
D_{1-}\Phi_6 &= i\Psi_{4-}, & D_{2+}\Phi_6 &= -i\Psi_{8+}, & D_{3+}\Phi_6 &= i\Psi_{2+}, & D_{4+}\Phi_6 &= -i\Psi_{3+},
\end{aligned}$$

$$\begin{aligned}
D_{1-}\Phi_7 &= i\Psi_{6-} , & D_{2+}\Phi_7 &= i\Psi_{2+} , & D_{3+}\Phi_7 &= i\Psi_{8+} , & D_{4+}\Phi_7 &= -i\Psi_{5+} , \\
D_{1-}\Phi_8 &= i\Psi_{7-} , & D_{2+}\Phi_8 &= i\Psi_{3+} , & D_{3+}\Phi_8 &= -i\Psi_{5+} , & D_{4+}\Phi_8 &= -i\Psi_{8+} , \\
D_{1-}\Psi_{1-} &= \partial_- \Phi_5 , & D_{2+}\Psi_{1-} &= \Phi_3 , & D_{3+}\Psi_{1-} &= \Phi_2 , & D_{4+}\Psi_{1-} &= \Phi_1 , \\
D_{1-}\Psi_{2+} &= \Phi_1 , & D_{2+}\Psi_{2+} &= \partial_+ \Phi_7 , & D_{3+}\Psi_{2+} &= \partial_+ \Phi_6 , & D_{4+}\Psi_{2+} &= -\partial_+ \Phi_5 , \\
D_{1-}\Psi_{3+} &= \Phi_2 , & D_{2+}\Psi_{3+} &= \partial_+ \Phi_8 , & D_{3+}\Psi_{3+} &= -\partial_+ \Phi_5 , & D_{4+}\Psi_{3+} &= -\partial_+ \Phi_6 , \\
D_{1-}\Psi_{4-} &= \partial_- \Phi_6 , & D_{2+}\Psi_{4-} &= \Phi_4 , & D_{3+}\Psi_{4-} &= -\Phi_1 , & D_{4+}\Psi_{4-} &= \Phi_2 , \\
D_{1-}\Psi_{5+} &= \Phi_3 , & D_{2+}\Psi_{5+} &= -\partial_+ \Phi_5 , & D_{3+}\Psi_{5+} &= -\partial_+ \Phi_8 , & D_{4+}\Psi_{5+} &= -\partial_+ \Phi_7 , \\
D_{1-}\Psi_{6-} &= \partial_- \Phi_7 , & D_{2+}\Psi_{6-} &= -\Phi_1 , & D_{3+}\Psi_{6-} &= -\Phi_4 , & D_{4+}\Psi_{6-} &= \Phi_3 , \\
D_{1-}\Psi_{7-} &= \partial_- \Phi_8 , & D_{2+}\Psi_{7-} &= -\Phi_2 , & D_{3+}\Psi_{7-} &= \Phi_3 , & D_{4+}\Psi_{7-} &= \Phi_4 , \\
D_{1-}\Psi_{8+} &= \Phi_4 , & D_{2+}\Psi_{8+} &= -\partial_+ \Phi_6 , & D_{3+}\Psi_{8+} &= \partial_+ \Phi_7 , & D_{4+}\Psi_{8+} &= -\partial_+ \Phi_8 .
\end{aligned} \tag{B.6}$$

Line color redefinitions below of the adinkras in Fig # 18 (b) through (d) create equivalent equations:

(b). Green $\rightarrow D_4$	(c.) Green $\rightarrow D_4$	(d.) Green $\rightarrow D_4$
Yellow $\rightarrow D_1$	Yellow $\rightarrow D_3$	Yellow $\rightarrow D_2$
	Red $\rightarrow D_1$	Red $\rightarrow D_3$
		Purple $\rightarrow D_1$

It is also very important to note that (e) - (g) correspond to $(p, q) = (2, 2)$ superfields. The adinkra in Fig # 18(e) has the associated equations,

$$\begin{aligned}
D_{1-}\Phi_1 &= i\partial_- \Psi_{3+} , & D_{2+}\Phi_1 &= -i\partial_+ \Psi_{7-} , & D_{3+}\Phi_1 &= i\partial_+ \Psi_{1-} , & D_{4-}\Phi_1 &= i\partial_- \Psi_{4+} , \\
D_{1-}\Phi_2 &= i\partial_- \Psi_{4+} , & D_{2+}\Phi_2 &= -i\partial_+ \Psi_{8-} , & D_{3+}\Phi_2 &= i\partial_+ \Psi_{2-} , & D_{4-}\Phi_2 &= -i\partial_- \Psi_{3+} , \\
D_{1-}\Phi_3 &= i\partial_- \Psi_{5+} , & D_{2+}\Phi_3 &= i\partial_+ \Psi_{1-} , & D_{3+}\Phi_3 &= i\partial_+ \Psi_{7-} , & D_{4-}\Phi_3 &= i\partial_- \Psi_{6+} , \\
D_{1-}\Phi_4 &= i\partial_- \Psi_{6+} , & D_{2+}\Phi_4 &= i\partial_+ \Psi_{2-} , & D_{3+}\Phi_4 &= i\partial_+ \Psi_{8-} , & D_{4-}\Phi_4 &= -i\partial_- \Psi_{5+} , \\
D_{1-}\Phi_5 &= i\Psi_{1-} , & D_{2+}\Phi_5 &= -i\Psi_{5+} , & D_{3+}\Phi_5 &= -i\Psi_{3+} , & D_{4-}\Phi_5 &= -i\Psi_{2-} , \\
D_{1-}\Phi_6 &= i\Psi_{2-} , & D_{2+}\Phi_6 &= -i\Psi_{6+} , & D_{3+}\Phi_6 &= -i\Psi_{4+} , & D_{4-}\Phi_6 &= i\Psi_{1-} , \\
D_{1-}\Phi_7 &= i\Psi_{7-} , & D_{2+}\Phi_7 &= i\Psi_{3+} , & D_{3+}\Phi_7 &= -i\Psi_{5+} , & D_{4-}\Phi_7 &= -i\Psi_{8-} , \\
D_{1-}\Phi_8 &= i\Psi_{8-} , & D_{2+}\Phi_8 &= i\Psi_{4+} , & D_{3+}\Phi_8 &= -i\Psi_{6+} , & D_{4-}\Phi_8 &= i\Psi_{7-} , \\
D_{1-}\Psi_{1-} &= \partial_- \Phi_5 , & D_{2+}\Psi_{1-} &= \Phi_3 , & D_{3+}\Psi_{1-} &= \Phi_1 , & D_{4-}\Psi_{1-} &= \partial_- \Phi_6 , \\
D_{1-}\Psi_{2-} &= \partial_- \Phi_6 , & D_{2+}\Psi_{2-} &= \Phi_4 , & D_{3+}\Psi_{2-} &= \Phi_2 , & D_{4-}\Psi_{2-} &= -\partial_- \Phi_5 , \\
D_{1-}\Psi_{3+} &= \Phi_1 , & D_{2+}\Psi_{3+} &= \partial_+ \Phi_7 , & D_{3+}\Psi_{3+} &= -\partial_+ \Phi_5 , & D_{4-}\Psi_{3+} &= -\Phi_2 , \\
D_{1-}\Psi_{4+} &= \Phi_2 , & D_{2+}\Psi_{4+} &= \partial_+ \Phi_8 , & D_{3+}\Psi_{4+} &= -\partial_+ \Phi_6 , & D_{4-}\Psi_{4+} &= \Phi_1 , \\
D_{1-}\Psi_{5+} &= \Phi_3 , & D_{2+}\Psi_{5+} &= -\partial_+ \Phi_5 , & D_{3+}\Psi_{5+} &= -\partial_+ \Phi_7 , & D_{4-}\Psi_{5+} &= -\Phi_4 , \\
D_{1-}\Psi_{6+} &= \Phi_4 , & D_{2+}\Psi_{6+} &= -\partial_+ \Phi_6 , & D_{3+}\Psi_{6+} &= -\partial_+ \Phi_8 , & D_{4-}\Psi_{6+} &= \Phi_3 ,
\end{aligned}$$

$$\begin{aligned}
D_{1-}\Psi_{7-} &= \partial_{-}\Phi_7 , & D_{2+}\Psi_{7-} &= -\Phi_1 , & D_{3+}\Psi_{7-} &= \Phi_3 , & D_{4-}\Psi_{7-} &= \partial_{-}\Phi_8 , \\
D_{1-}\Psi_{8-} &= \partial_{-}\Phi_8 , & D_{2+}\Psi_{8-} &= -\Phi_2 , & D_{3+}\Psi_{8-} &= \Phi_4 , & D_{4-}\Psi_{8-} &= -\partial_{-}\Phi_7 ,
\end{aligned}
\tag{B.7}$$

Similarly, redefining the colors below creates equivalent equations for the adinkras in Fig. # 19(f.) and (g.):

$$\begin{array}{ll}
\text{(f.) Green} \rightarrow D_3 & \text{(g.) Green} \rightarrow D_1 \\
\text{Yellow} \rightarrow D_1 & \text{Yellow} \rightarrow D_3 \\
\text{Red} \rightarrow D_4 & \text{Red} \rightarrow D_4
\end{array}$$

Appendix C: The $(p, q) = (2, 2)$ $(4|8|4)$ 2D Supermultiplet Is Not Two $(2|4|2)$ 2D Supermultiplets

In this appendix, we wish to examine more closely the $(p, q) = (2, 2)$ $(4|8|4)$ 2D supermultiplet defined by (B.7). For this purpose, let us re-examine a subset of the equations given by

$$\begin{aligned}
D_{1-}\Phi_5 &= i\Psi_{1-} , & D_{2+}\Phi_5 &= -i\Psi_{5+} , & D_{3+}\Phi_5 &= -i\Psi_{3+} , & D_{4-}\Phi_5 &= -i\Psi_{2-} , \\
D_{1-}\Phi_6 &= i\Psi_{2-} , & D_{2+}\Phi_6 &= -i\Psi_{6+} , & D_{3+}\Phi_6 &= -i\Psi_{4+} , & D_{4-}\Phi_6 &= i\Psi_{1-} , \\
D_{1-}\Phi_7 &= i\Psi_{7-} , & D_{2+}\Phi_7 &= i\Psi_{3+} , & D_{3+}\Phi_7 &= -i\Psi_{5+} , & D_{4-}\Phi_7 &= -i\Psi_{8-} , \\
D_{1-}\Phi_8 &= i\Psi_{8-} , & D_{2+}\Phi_8 &= i\Psi_{4+} , & D_{3+}\Phi_8 &= -i\Psi_{6+} , & D_{4-}\Phi_8 &= i\Psi_{7-} ,
\end{aligned}
\tag{C.1}$$

and eliminate all the fermions of negative helicity from these equations to obtain

$$D_{1-} \begin{bmatrix} \Phi_5 \\ \Phi_6 \\ \Phi_7 \\ \Phi_8 \end{bmatrix} = D_{4-} \begin{bmatrix} \Phi_6 \\ -\Phi_5 \\ \Phi_8 \\ -\Phi_7 \end{bmatrix} .
\tag{C.2}$$

Of course, we could also choose to eliminate the positive helicity fermions from (C.1) to obtain

$$D_{3+} \begin{bmatrix} \Phi_5 \\ \Phi_6 \\ \Phi_7 \\ \Phi_8 \end{bmatrix} = D_{2+} \begin{bmatrix} -\Phi_7 \\ -\Phi_8 \\ \Phi_5 \\ \Phi_6 \end{bmatrix} .
\tag{C.3}$$

These equations can be written more simply by introducing a four component vector defined by

$$\vec{\mathcal{A}} = \begin{bmatrix} \Phi_5 \\ \Phi_6 \\ \Phi_7 \\ \Phi_8 \end{bmatrix}, \quad (C.4)$$

which permits the results in (C.2) and (C.3) to be re-cast into the forms

$$D_{1-}\vec{\mathcal{A}} = i (\mathbf{I} \otimes \boldsymbol{\sigma}^2) D_{4-}\vec{\mathcal{A}}, \quad D_{3+}\vec{\mathcal{A}} = -i (\boldsymbol{\sigma}^2 \otimes \mathbf{I}) D_{2+}\vec{\mathcal{A}}, \quad (C.5)$$

or equivalently

$$D_{4-}\vec{\mathcal{A}} = -i (\mathbf{I} \otimes \boldsymbol{\sigma}^2) D_{1-}\vec{\mathcal{A}}, \quad D_{2+}\vec{\mathcal{A}} = i (\boldsymbol{\sigma}^2 \otimes \mathbf{I}) D_{3+}\vec{\mathcal{A}}. \quad (C.6)$$

where $(\mathbf{I} \otimes \boldsymbol{\sigma}^2)$ and $(\boldsymbol{\sigma}^2 \otimes \mathbf{I})$ are 4×4 matrices written in terms of the outer product of 2×2 matrices.

The equations in (C.5) and (C.6) are completely consistent with the $(p, q) = (2, 2)$ supersymmetry algebra. However, the real issue is whether the multiplet described by (B.6) can be equivalent to *two* copies of the multiplets described in (A.1). We believe the following argument show this is not possible.

Construct a quantity denoted by $\vec{\mathcal{B}}$ which is composed of two copies (an A copy and a B copy) of the fields associated with the lowest nodes in Fig. # 12 of the form

$$\vec{\mathcal{B}} = \begin{bmatrix} m_{11} & m_{12} & m_{13} & m_{14} \\ m_{21} & m_{22} & m_{23} & m_{24} \\ m_{31} & m_{32} & m_{33} & m_{34} \\ m_{41} & m_{42} & m_{43} & m_{44} \end{bmatrix} \begin{bmatrix} \Phi_3^{(A)} \\ \Phi_4^{(A)} \\ \Phi_3^{(B)} \\ \Phi_4^{(B)} \end{bmatrix} = \mathcal{M} \begin{bmatrix} \Phi_3^{(A)} \\ \Phi_4^{(A)} \\ \Phi_3^{(B)} \\ \Phi_4^{(B)} \end{bmatrix} \quad (C.7)$$

which introduces sixteen parameters $m_{11} \dots m_{44}$. If the $(4|8|4)$ supermultiplet is a linear combination of two $(2|4|2)$ mutlplets, then it should be possible to find a choice of the sixteen parameters such that $\vec{\mathcal{B}}$ satisfies the conditions in (C.5). In principle, this should be quite easy as there are only eight equations implied by the conditions in (C.5).

There are only two rows in (A.1) that are relevant for this analysis and for convenience we reproduce them below. For completeness of our analysis there is one other matter we must attend. We have established [11] that if one begins with an adinkra for a chiral multiplet, the adinkra for the twisted chiral multiplet is obtained by reversing signs for an odd number of the D-operators that appear in the D-equations. Picking

this to be the D_{3+} operator we can write upon eliminating the fermions between these equations

$$\begin{aligned} D_{1-}\Phi_3^{(A)} &= D_{4-}\Phi_4^{(A)} \quad , \quad D_{2+}\Phi_3^{(A)} = -\xi^{(A)} D_{3+}\Phi_4^{(A)} , \\ D_{1-}\Phi_4^{(A)} &= -D_{4-}\Phi_3^{(A)} , \quad D_{2+}\Phi_4^{(A)} = \xi^{(A)} D_{3+}\Phi_3^{(A)} , \end{aligned} \quad (C.8)$$

where the parameter $\xi^{(A)}$ satisfies $[\xi^{(A)}]^2 = 1$. For the chiral multiplet we choose $\xi^{(A)} = 1$ for the chiral multiplet and $\xi^{(A)} = -1$ for the twisted chiral multiplet. We now take (C.7) and (C.8) and check to see if the conditions in (C.5) can be satisfied by the sixteen parameters.

For the first condition in (C.5) we find

$$D_{1-}\vec{\mathcal{B}} = \mathcal{M} D_{1-} \begin{bmatrix} \Phi_3^{(A)} \\ \Phi_4^{(A)} \\ \Phi_3^{(B)} \\ \Phi_4^{(B)} \end{bmatrix} = \mathcal{M} D_{4-} \begin{bmatrix} \Phi_4^{(A)} \\ -\Phi_3^{(A)} \\ \Phi_4^{(B)} \\ -\Phi_3^{(B)} \end{bmatrix} = \mathcal{M} (\mathbf{I} \otimes i\sigma^2) D_{4-} \begin{bmatrix} \Phi_3^{(A)} \\ \Phi_4^{(A)} \\ \Phi_3^{(B)} \\ \Phi_4^{(B)} \end{bmatrix} . \quad (C.9)$$

Upon comparing the last formula for the result in (C.9) with the first result of (C.5), it is clear that \mathcal{M} must be chosen as the identity matrix. Using the fact that \mathcal{M} is the identity matrix we now calculate the second condition in (C.5) to find

$$\begin{aligned} D_{2+}\vec{\mathcal{B}} &= D_{2+} \begin{bmatrix} \Phi_3^{(A)} \\ \Phi_4^{(A)} \\ \Phi_3^{(B)} \\ \Phi_4^{(B)} \end{bmatrix} = D_{3+} \begin{bmatrix} -\xi^{(A)}\Phi_4^{(A)} \\ \xi^{(A)}\Phi_3^{(A)} \\ -\xi^{(B)}\Phi_4^{(B)} \\ \xi^{(B)}\Phi_3^{(B)} \end{bmatrix} \\ &= -\frac{1}{2}\xi^{(A)} ((\mathbf{I} + \sigma^3) \otimes i\sigma^2) D_{3+} \begin{bmatrix} \Phi_3^{(A)} \\ \Phi_4^{(A)} \\ \Phi_3^{(B)} \\ \Phi_4^{(B)} \end{bmatrix} \\ &\quad - \frac{1}{2}\xi^{(B)} ((\mathbf{I} - \sigma^3) \otimes i\sigma^2) D_{3+} \begin{bmatrix} \Phi_3^{(A)} \\ \Phi_4^{(A)} \\ \Phi_3^{(B)} \\ \Phi_4^{(B)} \end{bmatrix} \\ &= -\frac{1}{2} [\xi^{(A)} ((\mathbf{I} + \sigma^3) \otimes i\sigma^2) + \xi^{(B)} ((\mathbf{I} - \sigma^3) \otimes i\sigma^2)] D_{3+}\vec{\mathcal{B}} . \end{aligned} \quad (C.10)$$

It is manifest that for no choice of the ξ -parameters is it possible to satisfy the second condition in (C.5).

We thus conclude that the $(p, q) = (2, 2)$ $(4|8|4)$ 2D supermultiplet is a previously unobserved representation. Should this interpretation receive wider validation, this

discovery will provide further vindication for the program begun in 2001 and show the benefits of creating an algorithm that can systematically scan the zoo of 1D adinkras to find those that are liftable to 2D.

Appendix D: Mathematica Code for Scanning 2D Liftability of 1D Adinkras

Here we present the code used to determine liftable adinkras that have been presented in this work. We determine liftability using the valise $\mathcal{N} = 4$ adinkra found in AdinkraMat v.1.1. All calculations assume we start from that adinkra and raise or lower nodes from the positions shown in it. Nodes are labeled from left to right in the valise, just like in previous appendices. Thus, the far left fermion is labeled ψ_1 , and the far left boson is labeled ϕ_1 .

```
 $\beta_1 = 2;$ 
```

```
 $\beta_2 = 3;$ 
```

```
 $\beta_3 = 5;$ 
```

```
 $\beta_4 = 7;$ 
```

(* We used numbers instead of keeping these in symbolic notation to allow the computer to check equality (i.e. “==”) much faster than otherwise. These are prime numbers in order to differentiate $\beta_I\beta_J$ from $\beta_K\beta_L$ *)

```
TotalAdinkraNum = 247;
```

(*roughly the number of adinkras the code looks though*)

```
PsiDown = 0;
```

```
PsiUp = 1;
```

```
PhiBottom = -1;
```

```
PhiMid = 0;
```

```
PhiTop = 1;
```

```
GORP = ConstantArray[0, {7, 5, 8, TotalAdinkraNum}];
```

```
Evals = ConstantArray[0, {6, TotalAdinkraNum}];
```

```
LiftableAdinkraNum = ConstantArray[0, 54];
```

(*This array is used to find eigenvalues of the color matrices of every adinkra.

“54” is the number of (non-unique) liftable adinkras this code finds*)

```
RedOrange = 1;
OrangeRed = RedOrange;
RedGreen = 2;
GreenRed = RedGreen;
RedPurple = 3;
PurpleRed = RedPurple;
OrangeGreen = 4;
GreenOrange = OrangeGreen;
OrangePurple = 5;
PurpleOrange = OrangePurple;
GreenPurple = 6;
PurpleGreen = GreenPurple;
(*These are used when recording an adinkra's associated
color matrix eigenvalues, to make the indices easier to read*)
```

```
AdinkraNum = 0;
(*Counts the number of adinkras the code has so far seen
within the For loops below*)
bottomnodeDown = 0;
bottomnodeUp = 1;
topnodeUp = 0;
topnodeDown = 1;
numLiftable = 0; (*Counts the number of liftable
adinkras the code has seen in the For loops*)
For[ $\psi1 = \text{PsiDown}$ ,  $\psi1 \leq \text{PsiUp}$ ,  $\psi1++$ ,
For[ $\psi2 = \text{PsiDown}$ ,  $\psi2 \leq \text{PsiUp}$ ,  $\psi2++$ ,
For[ $\psi3 = \text{PsiDown}$ ,  $\psi3 \leq \text{PsiUp}$ ,  $\psi3++$ ,
For[ $\psi4 = \text{PsiDown}$ ,  $\psi4 \leq \text{PsiUp}$ ,  $\psi4++$ ,
```

(*all the rest stay put/attached to $\phi1$ *)

```
For[ $\psi5 = \text{PsiDown}$ ,  $\psi5 \leq \text{PsiUp}$ ,  $\psi5++$ ,
```

(*move only 1 level*)

For[$\psi_6 = \text{PsiDown}, \psi_6 \leq \text{PsiUp}, \psi_6++$,
 For[$\psi_7 = \text{PsiDown}, \psi_7 \leq \text{PsiUp}, \psi_7++$,
 For[$\psi_8 = \text{PsiDown}, \psi_8 \leq \text{PsiUp}, \psi_8++$,
 For[$\phi_1 = \text{PhiBottom}, \phi_1 \leq \text{PhiTop}, \phi_1++$,

(* ϕ_8 stays put, only ϕ_1 goes up*)

For[$\phi_2 = \text{PhiBottom}, \phi_2 \leq \text{PhiTop}, \phi_2++$,
 For[$\phi_3 = \text{PhiBottom}, \phi_3 \leq \text{PhiTop}, \phi_3++$,
 For[$\phi_4 = \text{PhiBottom}, \phi_4 \leq \text{PhiTop}, \phi_4++$,
 For[$\phi_5 = \text{PhiBottom}, \phi_5 \leq \text{PhiTop}, \phi_5++$,
 For[$\phi_6 = \text{PhiBottom}, \phi_6 \leq \text{PhiTop}, \phi_6++$,
 For[$\phi_7 = \text{PhiBottom}, \phi_7 \leq \text{PhiTop}, \phi_7++$,
 For[$\phi_8 = \text{PhiBottom}, \phi_8 \leq \text{PhiTop}, \phi_8++$,

(*This is equivalent to using Einstein notation for clarity)

For[$\psi_I = \text{PsiDown}, \psi_I \leq \text{PsiUp}, \psi_I++$,
 For[$\phi_J = \text{PhiBottom}, \phi_J \leq \text{PhiTop}, \phi_J++$,

(* Basically we use many for loops to either raise the fermion nodes, which are on the bottom row, denoted as ψ_{up} , or we keep them on the bottom row (ψ_{down}). Similarly, we can lower a boson node (ϕ_{down}), keep it on the same row (ϕ_{Mid}) or raise this node if that is allowed (ϕ_{up}). Knowing when it is valise or not is determined by a massive if statement made at the beginning of the for loop: *)

(*Labels to make the If statement readable*)

$\psi_{\text{Middle}} = (\psi_1 == \text{PsiDown} \ \&\& \ \psi_2 == \text{PsiDown} \ \&\& \ \psi_3 == \text{PsiDown} \ \&\& \ \psi_4 == \text{PsiDown} \ \&\& \ \psi_5 == \text{PsiDown} \ \&\& \ \psi_6 == \text{PsiDown} \ \&\&$

$\psi_7 == \text{PsiDown} \ \&\& \ \psi_8 == \text{PsiDown})$;
 $\text{NoPhiOnTop} = (\phi_1 \neq \text{PhiTop} \ \&\& \ \phi_2 \neq \text{PhiTop} \ \&\& \ \phi_3 \neq \text{PhiTop} \ \&\& \ \phi_4 \neq \text{PhiTop} \ \&\& \ \phi_5 \neq \text{PhiTop} \ \&\& \ \phi_6 \neq \text{PhiTop} \ \&\& \ \phi_7 \neq \text{PhiTop} \ \&\& \ \phi_8 \neq \text{PhiTop})$;

$\psi_{\text{all}} = \psi_1 + \psi_2 + \psi_3 + \psi_4 + \psi_5 + \psi_6 + \psi_7 + \psi_8$;

$$\text{all}\phi = \phi1 + \phi2 + \phi3 + \phi4 + \phi5 + \phi6 + \phi7 + \phi8;$$

$$\phi1\psi s = (\psi1 + \psi2 + \psi3 + \psi5);$$

$$\phi2\psi s = (\psi1 + \psi2 + \psi4 + \psi6);$$

$$\phi3\psi s = (\psi1 + \psi3 + \psi4 + \psi7);$$

$$\phi4\psi s = (\psi2 + \psi3 + \psi4 + \psi8);$$

$$\phi5\psi s = (\psi1 + \psi5 + \psi6 + \psi7);$$

$$\phi6\psi s = (\psi2 + \psi5 + \psi6 + \psi8);$$

$$\phi7\psi s = (\psi3 + \psi5 + \psi7 + \psi8);$$

$$\phi8\psi s = (\psi4 + \psi6 + \psi7 + \psi8);$$

(*Impossible cases:

- 1) if lowest boson is on the bottom but the fermion nodes above it move
- 2) if the highest boson is on the top but the fermion nodes below it move

Due to the symmetry of the adinkras, we need to look at a small fraction of the total number of raised and lowered nodes. *)

If[

$$(\phi1 == \text{PhiBottom} \ \&\& \ \psi\text{Middle} \ \&\& \ \text{NoPhiOnTop})$$

(*This is equivalent to

keeping the first boson on the bottom row, and moving the other fermions above or below a single row of fermions.

In other words we look into the liftability of (1|8|7)

adinkras, (2|8|6) adinkras, etc. up to (4|8|4) adinkras*)

||(

((*1 boson down*)

(*Here we keep the a boson node, ϕ_i ,

on the bottom, while raising and lowering fermion nodes*)

$$(\phi1\psi s == 4 * \text{PsiDown} \ \&\& \ \phi1 == \text{PhiBottom}$$

$$\ \&\& \ \text{NoPhiOnTop} \ \&\& \ \text{all}\phi == 1 * \text{PhiBottom})$$

$$\|(\phi2\psi s == 4 * \text{PsiDown} \ \&\& \ \phi2 == \text{PhiBottom}$$

$$\ \&\& \ \text{NoPhiOnTop} \ \&\& \ \text{all}\phi == 1 * \text{PhiBottom})$$

$$\|(\phi3\psi s == 4 * \text{PsiDown} \ \&\& \ \phi3 == \text{PhiBottom}$$

$$\ \&\& \ \text{NoPhiOnTop} \ \&\& \ \text{all}\phi == 1 * \text{PhiBottom})$$

$\|(\phi 4 \psi_s == 4 * \text{PsiDown} \ \&\& \ \phi 4 == \text{PhiBottom}$
 $\ \&\& \ \text{NoPhiOnTop} \ \&\& \ \text{all}\phi == 1 * \text{PhiBottom})$
 $)$
 (*In this case, at least one fermion is raised*)
 $\&\& \ \psi_{\text{all}} \geq 1 * \text{PsiUp})$

$\|$
 $($
 $($
 $(\phi 5 \psi_s == 4 * \text{PsiDown} \ \&\& \ \phi 5 == \text{PhiBottom}$
 $\ \&\& \ \text{NoPhiOnTop} \ \&\& \ \text{all}\phi == 1 * \text{PhiBottom})$
 $\|(\phi 6 \psi_s == 4 * \text{PsiDown} \ \&\& \ \phi 6 == \text{PhiBottom}$
 $\ \&\& \ \text{NoPhiOnTop} \ \&\& \ \text{all}\phi == 1 * \text{PhiBottom})$
 $\|(\phi 7 \psi_s == 4 * \text{PsiDown} \ \&\& \ \phi 7 == \text{PhiBottom}$
 $\ \&\& \ \text{NoPhiOnTop} \ \&\& \ \text{all}\phi == 1 * \text{PhiBottom})$
 $\|(\phi 8 \psi_s == 4 * \text{PsiDown} \ \&\& \ \phi 8 == \text{PhiBottom}$
 $\ \&\& \ \text{NoPhiOnTop} \ \&\& \ \text{all}\phi == 1 * \text{PhiBottom})$
 $)$
 (*In this case, to avoid repeating adinkras,
 we have at least 2 fermion nodes raised*)
 $\&\& \ (\psi_{\text{all}} \geq 2 * \text{PsiUp})$

$)$

$\|$
 $($
 $($
 $($
 $(*2 \text{ bosons down}*)$
 $($
 $(*We have exactly 2 boson nodes down,$
 $\text{and 2 fermion nodes up. All possible combinations are below}*)$
 $(\phi 1 \psi_s == 4 * \text{PsiDown} \ \&\& \ \phi 1 == \text{PhiBottom})$
 $\|(\phi 2 \psi_s == 4 * \text{PsiDown} \ \&\& \ \phi 2 == \text{PhiBottom})$
 $)$
 $\&\&$
 $($
 $(\phi 3 \psi_s == 4 * \text{PsiDown} \ \&\& \ \phi 3 == \text{PhiBottom})$


```

||(\phi4\psi == 4 * PsiDown && \phi4 == PhiBottom)
||(\phi5\psi == 4 * PsiDown && \phi5 == PhiBottom)
||(\phi6\psi == 4 * PsiDown && \phi6 == PhiBottom)
||(\phi7\psi == 4 * PsiDown && \phi7 == PhiBottom)
||(\phi8\psi == 4 * PsiDown && \phi8 == PhiBottom)
)
&& NoPhiOnTop && all\phi == 2 * PhiBottom
)

||(
(
(*The fully extended tesseract based adinkra
(i.e. the real scalar supermultiplet) is included with this statement.*)
(\phi1\psi == 4 * PsiDown && \phi1 == PhiBottom)
&& (\phi2\psi == 4 * PsiDown && \phi2 == PhiBottom)
&& NoPhiOnTop && all\phi == 2 * PhiBottom))
)

(*Exactly 2 fermion nodes are up
&& \psiall==2 * PsiUp
)
||(
(*2 boson nodes on the bottom row, and
1 or 2 fermion nodes raised and lowered*)
\phi1 == PhiBottom && \phi1\psi == 4 * PsiDown
&& \phi8 == PhiTop && \phi8\psi == 4 * PsiUp
&& (Abs[\phi2] + Abs[\phi3] + Abs[\phi4]
+ Abs[\phi5] + Abs[\phi6] + Abs[\phi7]) == 6 * PhiMid
)
||(
\phi2 == PhiBottom && \phi2\psi == 4 * PsiDown
&& \phi7 == PhiTop && \phi7\psi == 4 * PsiUp
&& (Abs[\phi1] + Abs[\phi3] + Abs[\phi4]
+ Abs[\phi5] + Abs[\phi6] + Abs[\phi8]) == 6 * PhiMid
)
||(
\phi3 == PhiBottom && \phi3\psi == 4 * PsiDown

```

```

&&  $\phi_6 == \text{PhiTop}$  &&  $\phi_6\psi_s == 4 * \text{PsiUp}$ 
&& ( $\text{Abs}[\phi_1] + \text{Abs}[\phi_2] + \text{Abs}[\phi_4]$ 
+  $\text{Abs}[\phi_5] + \text{Abs}[\phi_7] + \text{Abs}[\phi_8]$ ) ==  $6 * \text{PhiMid}$ 
)
||(
 $\phi_4 == \text{PhiBottom}$  &&  $\phi_4\psi_s == 4 * \text{PsiDown}$ 
&&  $\phi_5 == \text{PhiTop}$  &&  $\phi_5\psi_s == 4 * \text{PsiUp}$ 
&& ( $\text{Abs}[\phi_1] + \text{Abs}[\phi_2] + \text{Abs}[\phi_3]$ 
+  $\text{Abs}[\phi_6] + \text{Abs}[\phi_7] + \text{Abs}[\phi_8]$ ) ==  $6 * \text{PhiMid}$ 
)

```

(*Below we define the color matrices \mathcal{B}_{iL} and \mathcal{B}_{jR} for every adinkra*)

```

greenL = ConstantArray[0, {8, 8}];
orangeL = ConstantArray[0, {8, 8}];
redL = ConstantArray[0, {8, 8}];
purpleL = ConstantArray[0, {8, 8}];

```

```

greenR = ConstantArray[0, {8, 8}];
orangeR = ConstantArray[0, {8, 8}];
redR = ConstantArray[0, {8, 8}];
purpleR = ConstantArray[0, {8, 8}];

```

```

PosMat = ConstantArray[0, {5, 8}];

```

(*The below code makes the color matrices, and position matrix (PosMat). Here the position matrix shows the relative position of fermion and boson nodes by raising or lowering nodes from the $\mathcal{N} = 4$ valise adinkra in AdinkraMat v. 1.1. Thus a position matrix:

$$\begin{pmatrix} 0 & 0 & 0 & 0 & 0 & 0 & 0 & 0 & 0 \\ 0 & 0 & 0 & 0 & 0 & 0 & 0 & 0 & 0 \\ 0 & 0 & 0 & 0 & 1 & 1 & 1 & 1 & 1 \\ i & i & i & i & i & i & i & i & i \\ 1 & 1 & 1 & 1 & 0 & 0 & 0 & 0 & 0 \end{pmatrix}$$

represents the 4 boson nodes, ϕ_5 , ϕ_6 , ϕ_7 , and ϕ_8 on the top row, with all the other boson nodes on the bottom row. The fermions are all in the center row.

To make the code need fewer for loops, I added ϕ and/or ψ together. Hence, if ϕ_8 is

above ψ_8 , then the code knows that “ $\phi_8 + \psi_8 = \text{PsiDown} + \text{PhiMid} = 0$ ”, which implies the color matrices’ elements for that node are β_i^{+1} .

*)

(* ψ_8 *)

purpleL[[8, 4]] = $\beta_4 \wedge ((-1) \wedge (\psi_8 + \phi_4)); (*\text{connects to } \phi_4^*)$
redL[[8, 6]] = $\beta_3 \wedge ((-1) \wedge (\psi_8 + \phi_6)); (*\text{connects to } \phi_6^*)$
orangeL[[8, 7]] = $\beta_2 \wedge ((-1) \wedge (\psi_8 + \phi_7)); (*\text{connects to } \phi_7^*)$
greenL[[8, 8]] = $\beta_1 \wedge ((-1) \wedge (\phi_8 + \psi_8)); (*\text{connects to } \phi_8^*)$
PosMat[[4 - 2* ψ_8 , 8]] = i ;

(* ψ_7 *)

purpleL[[7, 3]] = $\beta_4 \wedge ((-1) \wedge (\phi_3 + \psi_7)); (*\text{connects to } \phi_3^*)$
redL[[7, 5]] = $\beta_3 \wedge ((-1) \wedge (\phi_5 + \psi_7)); (*\text{connects to } \phi_5^*)$
greenL[[7, 7]] = $\beta_1 \wedge ((-1) \wedge (\phi_7 + \psi_7)); (*\text{connects to } \phi_7^*)$
orangeL[[7, 8]] = $\beta_2 \wedge ((-1) \wedge (\phi_8 + \psi_7)); (*\text{connects to } \phi_8^*)$
PosMat[[4 - 2* ψ_7 , 7]] = i ;

(* ψ_6 *)

purpleL[[6, 2]] = $\beta_4 \wedge ((-1) \wedge (\phi_2 + \psi_6)); (*\text{connects to } \phi_2^*)$
orangeL[[6, 5]] = $\beta_2 \wedge ((-1) \wedge (\phi_5 + \psi_6)); (*\text{connects to } \phi_5^*)$
greenL[[6, 6]] = $\beta_1 \wedge ((-1) \wedge (\phi_6 + \psi_6)); (*\text{connects to } \phi_6^*)$
redL[[6, 8]] = $\beta_3 \wedge ((-1) \wedge (\phi_8 + \psi_6)); (*\text{connects to } \phi_8^*)$
PosMat[[4 - 2* ψ_6 , 6]] = i ;

(* ψ_5 *)

purpleL[[5, 1]] = $\beta_4 \wedge ((-1) \wedge (\phi_1 + \psi_5)); (*\text{connects to } \phi_1^*)$
greenL[[5, 5]] = $\beta_1 \wedge ((-1) \wedge (\phi_5 + \psi_5)); (*\text{connects to } \phi_5^*)$
orangeL[[5, 6]] = $\beta_2 \wedge ((-1) \wedge (\phi_6 + \psi_5)); (*\text{connects to } \phi_6^*)$
redL[[5, 7]] = $\beta_3 \wedge ((-1) \wedge (\phi_7 + \psi_5)); (*\text{connects to } \phi_7^*)$
PosMat[[4 - 2* ψ_5 , 5]] = i ;

(* ψ_4 *)

redL[[4, 2]] = $\beta_3 \wedge ((-1) \wedge (\psi_4 + \phi_2)); (*\text{connects to } \phi_2^*)$
orangeL[[4, 3]] = $\beta_2 \wedge ((-1) \wedge (\psi_4 + \phi_3)); (*\text{connects to } \phi_3^*)$
greenL[[4, 4]] = $\beta_1 \wedge ((-1) \wedge (\psi_4 + \phi_4)); (*\text{connects to } \phi_4^*)$
purpleL[[4, 8]] = $\beta_4 \wedge ((-1) \wedge (\phi_8 + \psi_4)); (*\text{connects to } \phi_8^*)$

$$\text{PosMat}[[4 - 2*\psi 4, 4]] = i;$$

$$(*\psi 3^*)$$

$$\text{redL}[[3, 1]] = \beta 3 \wedge ((-1) \wedge (\phi 1 + \psi 3)); (*\text{connects to } \phi 1^*)$$

$$\text{greenL}[[3, 3]] = \beta 1 \wedge ((-1) \wedge (\psi 3 + \phi 3)); (*\text{connects to } \phi 3^*)$$

$$\text{orangeL}[[3, 4]] = \beta 2 \wedge ((-1) \wedge (\psi 3 + \phi 4)); (*\text{connects to } \phi 4^*)$$

$$\text{purpleL}[[3, 7]] = \beta 4 \wedge ((-1) \wedge (\psi 3 + \phi 7)); (*\text{connects to } \phi 7^*)$$

$$\text{PosMat}[[4 - 2*\psi 3, 3]] = i;$$

$$(*\psi 2^*)$$

$$\text{orangeL}[[2, 1]] = \beta 2 \wedge ((-1) \wedge (\psi 2 + \phi 1)); (*\text{connects to } \phi 1^*)$$

$$\text{greenL}[[2, 2]] = \beta 1 \wedge ((-1) \wedge (\psi 2 + \phi 2)); (*\text{connects to } \phi 2^*)$$

$$\text{redL}[[2, 4]] = \beta 3 \wedge ((-1) \wedge (\psi 2 + \phi 4)); (*\text{connects to } \phi 4^*)$$

$$\text{purpleL}[[2, 6]] = \beta 4 \wedge ((-1) \wedge (\psi 2 + \phi 6)); (*\text{connects to } \phi 6^*)$$

$$\text{PosMat}[[4 - 2*\psi 2, 2]] = i;$$

$$(*\psi 1^*)$$

$$\text{greenL}[[1, 1]] = \beta 1 \wedge ((-1) \wedge (\phi 1 + \psi 1)); (*\text{connects to } \phi 1^*)$$

$$\text{orangeL}[[1, 2]] = \beta 2 \wedge ((-1) \wedge (\psi 1 + \phi 2)); (*\text{connects to } \phi 2^*)$$

$$\text{redL}[[1, 3]] = \beta 3 \wedge ((-1) \wedge (\psi 1 + \phi 3)); (*\text{connects to } \phi 3^*)$$

$$\text{purpleL}[[1, 5]] = \beta 4 \wedge ((-1) \wedge (\psi 1 + \phi 5)); (*\text{connects to } \phi 5^*)$$

$$\text{PosMat}[[4 - 2*\psi 1, 1]] = i;$$

$$(*\phi 8^*)$$

$$\text{greenR}[[8, 8]] = \beta 1 \wedge ((-1) \wedge (1 + \phi 8 + \psi 8)); (*\text{connects to } \psi 8^*)$$

$$\text{orangeR}[[8, 7]] = \beta 2 \wedge ((-1) \wedge (1 + \phi 8 + \psi 7)); (*\text{connects to } \psi 7^*)$$

$$\text{redR}[[8, 6]] = \beta 3 \wedge ((-1) \wedge (1 + \phi 8 + \psi 6)); (*\text{connects to } \psi 6^*)$$

$$\text{purpleR}[[8, 4]] = \beta 4 \wedge ((-1) \wedge (1 + \phi 8 + \psi 4)); (*\text{connects to } \psi 4^*)$$

$$\text{PosMat}[[3 - 2*\phi 8, 8]] = 1;$$

$$(*\phi 7^*)$$

$$\text{greenR}[[7, 7]] = \beta 1 \wedge ((-1) \wedge (1 + \phi 7 + \psi 7)); (*\text{connects to } \psi 7^*)$$

$$\text{orangeR}[[7, 8]] = \beta 2 \wedge ((-1) \wedge (\psi 8 + 1 + \phi 7)); (*\text{connects to } \psi 8^*)$$

$$\text{purpleR}[[7, 3]] = \beta 4 \wedge ((-1) \wedge (\psi 3 + 1 + \phi 7)); (*\text{connects to } \psi 3^*)$$

$$\text{redR}[[7, 5]] = \beta 3 \wedge ((-1) \wedge (\psi 5 + 1 + \phi 7)); (*\text{connects to } \psi 5^*)$$

$$\text{PosMat}[[3 - 2*\phi 7, 7]] = 1;$$

(* $\phi 6^*$)

greenR[[6, 6]] = $\beta 1 \wedge ((-1) \wedge (1 + \phi 6 + \psi 6))$;(*connects to $\psi 6^*$)
redR[[6, 8]] = $\beta 3 \wedge ((-1) \wedge (\psi 8 + 1 + \phi 6))$;(*connects to $\psi 8^*$)
purpleR[[6, 2]] = $\beta 4 \wedge ((-1) \wedge (\psi 2 + 1 + \phi 6))$;(*connects to $\psi 2^*$)
orangeR[[6, 5]] = $\beta 2 \wedge ((-1) \wedge (\psi 5 + 1 + \phi 6))$;(*connects to $\psi 5^*$)
PosMat[[3 - 2* $\phi 6$, 6]] = 1;

(* $\phi 5^*$)

orangeR[[5, 6]] = $\beta 2 \wedge ((-1) \wedge (\psi 6 + 1 + \phi 5))$;(*connects to $\psi 6^*$)
redR[[5, 7]] = $\beta 3 \wedge ((-1) \wedge (\psi 7 + 1 + \phi 5))$;(*connects to $\psi 7^*$)
purpleR[[5, 1]] = $\beta 4 \wedge ((-1) \wedge (\psi 1 + 1 + \phi 5))$;(*connects to $\psi 1^*$)
greenR[[5, 5]] = $\beta 1 \wedge ((-1) \wedge (1 + \phi 5 + \psi 5))$;(*connects to $\psi 5^*$)
PosMat[[3 - 2* $\phi 5$, 5]] = 1;

(* $\phi 4^*$)

orangeR[[4, 3]] = $\beta 2 \wedge ((-1) \wedge (1 + \phi 4 + \psi 3))$;(*connects to $\psi 3^*$)
redR[[4, 2]] = $\beta 3 \wedge ((-1) \wedge (1 + \phi 4 + \psi 2))$;(*connects to $\psi 2^*$)
purpleR[[4, 8]] = $\beta 4 \wedge ((-1) \wedge (\psi 8 + 1 + \phi 4))$;(*connects to $\psi 8^*$)
greenR[[4, 4]] = $\beta 1 \wedge ((-1) \wedge (1 + \phi 4 + \psi 4))$;(*connects to $\psi 4^*$)
PosMat[[3 - 2* $\phi 4$, 4]] = 1;

(* $\phi 3^*$)

greenR[[3, 3]] = $\beta 1 \wedge ((-1) \wedge (1 + \phi 3 + \psi 3))$;(*connects to $\psi 3^*$)
redR[[3, 1]] = $\beta 3 \wedge ((-1) \wedge (\psi 1 + 1 + \phi 3))$;(*connects to $\psi 1^*$)
purpleR[[3, 7]] = $\beta 4 \wedge ((-1) \wedge (1 + \phi 3 + \psi 7))$;(*connects to $\psi 7^*$)
orangeR[[3, 4]] = $\beta 2 \wedge ((-1) \wedge (1 + \phi 3 + \psi 4))$;(*connects to $\psi 4^*$)
PosMat[[3 - 2* $\phi 3$, 3]] = 1;

(* $\phi 2^*$)

greenR[[2, 2]] = $\beta 1 \wedge ((-1) \wedge (1 + \phi 2 + \psi 2))$;(*connects to $\psi 2^*$)
orangeR[[2, 1]] = $\beta 2 \wedge ((-1) \wedge (1 + \phi 2 + \psi 1))$;(*connects to $\psi 1^*$)
purpleR[[2, 6]] = $\beta 4 \wedge ((-1) \wedge (1 + \phi 2 + \psi 6))$;(*connects to $\psi 6^*$)
redR[[2, 4]] = $\beta 3 \wedge ((-1) \wedge (1 + \phi 2 + \psi 4))$;(*connects to $\psi 4^*$)
PosMat[[3 - 2* $\phi 2$, 2]] = 1;

(* $\phi 1^*$)

greenR[[1, 1]] = $\beta 1 \wedge ((-1) \wedge (1 + \phi 1 + \psi 1))$;(*connects to $\psi 1^*$)

```

orangeR[[1, 2]] =  $\beta_2 \wedge ((-1) \wedge (1 + \phi_1 + \psi_2))$ ;(*connects to  $\psi_2$ *)
redR[[1, 3]] =  $\beta_3 \wedge ((-1) \wedge (1 + \phi_1 + \psi_3))$ ;(*connects to  $\psi_3$ *)
purpleR[[1, 5]] =  $\beta_4 \wedge ((-1) \wedge (1 + \phi_1 + \psi_5))$ ;(*connects to  $\psi_5$ *)
PosMat[[3 - 2* $\phi_1$ , 1]] = 1;

```

```

AdinkraNum++;(*Counts the number of adinkras we have looked through*)

```

(*We organizing all the matrices into an array, GORP, which is an acronym for the line colors. Once all liftable adinkras are found, one may glean all necessary information of an adinkra by plugging in its associated number into the “AdinkraNum” index of GORP.*)

```

GORP[[1, All, All, AdinkraNum]] = PosMat;
GORP[[2, All, All, AdinkraNum]] = redL.orangeR;
GORP[[3, All, All, AdinkraNum]] = redL.greenR;
GORP[[4, All, All, AdinkraNum]] = redL.purpleR;
GORP[[5, All, All, AdinkraNum]] = orangeL.greenR;
GORP[[6, All, All, AdinkraNum]] = orangeL.purpleR;
GORP[[7, All, All, AdinkraNum]] = greenL.purpleR;

```

(*Eigenvalues of color matrices used to find bow ties*)

```

Evals[[RedOrange, AdinkraNum]] = Eigenvalues[redL.orangeR];
Evals[[RedGreen, AdinkraNum]] = Eigenvalues[redL.greenR];
Evals[[RedPurple, AdinkraNum]] = Eigenvalues[redL.purpleR];
Evals[[OrangeGreen, AdinkraNum]] = Eigenvalues[orangeL.greenR];
Evals[[OrangePurple, AdinkraNum]] = Eigenvalues[orangeL.purpleR];
Evals[[GreenPurple, AdinkraNum]] = Eigenvalues[greenL.purpleR];
(*)

```

When determining liftability, we remember that, If color i and j form bow ties, then we put the colors in a set S. for any other color - if it forms bow ties with colors in S, then it is also in S.

If there exists a color (or colors) not in S (i.e. in another set S') then the adinkra is liftable

*)

```

BowTies = ConstantArray[False, 6];
(*Here we check if the given color combo forms any bow ties. *)
For[ColorCombo = 1, ColorCombo ≤ 6, ColorCombo++,
  For[evalIndex = 1, evalIndex ≤ Dimensions[Evals[[ColorCombo, AdinkraNum]]][[1]],
    evalIndex++,
    (*Two color bow tie formed. put both colors in the set BowTies:
      1: red-orange
      2: red-green
      3: red-purple
      4: orange-green
      5:orange-purple
      6:green-purple
    *)
    If[Abs[Evals[[ColorCombo, AdinkraNum]][[evalIndex]]] ≠ 1,
      BowTies[[ColorCombo]] = True;
      Break[];
    ] ] ]

```

(*Cases when the adinkras are liftable:

```

1: Green colored lines are bow tie free
2: Orange colored lines are bow tie free
3: Red colored lines are bow tie free
4:Purple colored lines are bow tie free
5: Only red-orange and green-purple bow ties
6: Only red-purple and green-orange bow ties
7: Only red-green and orange-purple bow ties
*)

```

```

If[(*case 1*)
BowTies[[GreenRed]] == False
&& BowTies[[GreenOrange]] == False
&& BowTies[[GreenPurple]] == False,
  numLiftable++;(*Here we count the number of
                  (un-unique) liftable adinkras found so far*)
  LiftableAdinkraNum[[numLiftable]] = AdinkraNum;
  (*Here we put the liftable

```

adinkra's label into a convenient array*)

```
Break[];  
]
```

```
If>(*case 2*)  
BowTies[[OrangeRed]] == False  
&& BowTies[[OrangeGreen]] == False  
&& BowTies[[OrangePurple]] == False,  
  numLiftable++;  
  LiftableAdinkraNum[[numLiftable]] = AdinkraNum;  
  Break[];  
]
```

```
If>(*case 3*)  
BowTies[[RedGreen]] == False  
&& BowTies[[RedOrange]] == False  
&& BowTies[[RedPurple]] == False,  
  numLiftable++;  
  LiftableAdinkraNum[[numLiftable]] = AdinkraNum;  
  Break[];  
]
```

```
If>(*case 4*)  
BowTies[[PurpleRed]] == False  
&& BowTies[[PurpleOrange]] == False  
&& BowTies[[PurpleGreen]] == False,  
  numLiftable++;  
  LiftableAdinkraNum[[numLiftable]] = AdinkraNum;  
  Break[];  
]
```

```
If>(*case 5*)  
BowTies[[RedOrange]] == True  
&& BowTies[[GreenPurple]] == True  
&& Sum[BowTies[[ii]], {ii, 1, 6}] == 2*True + 4*False,  
  numLiftable++;  
  LiftableAdinkraNum[[numLiftable]] = AdinkraNum;
```


-If the eigenvalues are the same, ignore (we found that knowing the total number of bowties can go a long way to determining whether two adinkras are the same).

*)

```

TotalUniqueAdinkras = 1;
(*LiftableAdinkraNum[[1]]*)
UniqueAdinkraNum = ConstantArray[0, 18];
UniqueAdinkraNum[[1]] = LiftableAdinkraNum[[1]];

For[i = 2, i ≤ numLiftable, i++,
  count = 0;(*We use this variable to determine whether an adinkra is unique*)
  For[j = 1, j ≤ TotalUniqueAdinkras, j++,
    NewAdnk =
      Sort[Join[Evals[[1, LiftableAdinkraNum[[i]]]],
        Evals[[2, LiftableAdinkraNum[[i]]]],
        Evals[[3, LiftableAdinkraNum[[i]]]],
        Evals[[4, LiftableAdinkraNum[[i]]]],
        Evals[[5, LiftableAdinkraNum[[i]]]],
        Evals[[6, LiftableAdinkraNum[[i]]]]];
    OldAdnk =
      Sort[Join[Evals[[1, UniqueAdinkraNum[[j]]]],
        Evals[[2, UniqueAdinkraNum[[j]]]],
        Evals[[3, UniqueAdinkraNum[[j]]]],
        Evals[[4, UniqueAdinkraNum[[j]]]],
        Evals[[5, UniqueAdinkraNum[[j]]]],
        Evals[[6, UniqueAdinkraNum[[j]]]]];
    If[ NewAdnk == OldAdnk,
      Break[];
      (*If not the same as the previous adinkra*)
      count++;
    ]
  ]
]
(*If unique*)
If[count == TotalUniqueAdinkras,
  TotalUniqueAdinkras++;

```

UniqueAdinkraNum[[TotalUniqueAdinkras]] = LifiableAdinkraNum[[i]];
]

References

- [1] Y. A. Gelfand and E. P. Likhtman, “Extension of the Algebra of Poincare Group Generators and Violation of p Invariance,” JETP Lett. **13** (1971) 323; D. Volkov and V. Akulov, “Is the Neutrino a Goldstone Particle?,” Phys. Lett. **B46** (1973) 109; J. Wess and B. Zumino, “Supergauge Transformations in Four-Dimensions,” Nucl. Phys. **B70** (1974) 39; *ibid.* “Supergauge Invariant Extension of Quantum Electrodynamics,” **B78** (1974) 1; *ibid.* A Lagrangian Model Invariant Under Supergauge Transformations, Phys. Lett. **B49** (1974) 52.
- [2] S. Ferrara, J. Wess, and B. Zumino, “Supergauge Multiplets and Superfields,” Phys. Lett. **B51** (1974) 239; A. Salam, and J. A. Strathdee, “On Superfields and Fermi-Bose Symmetry,” Phys. Rev. **D11** D11 (1975) 1521.
- [3] M. Faux, S. J. Gates, Jr., “Adinkras: A Graphical Technology for Supersymmetric Representation Theory, Phys. Rev. D71 (2005) 065002, arXiv:0408004.
- [4] S. J. Gates, Jr., W. D. Linch, III, and J. Phillips, “When Superspace Is Not Enough, Univ. of Maryland preprint UMDEPP-02-054, Caltech preprint CALT-68-2387, hep-th/0211034 [hep-th], unpublished.
- [5] M. G. Faux, K. M. Iga, and G. D. Landweber, “Dimensional Enhancement via Supersymmetry, Adv. Math. Phys. 2011 (2011) **259089**, arXiv:0907.3605 [hep-th]; M. G. Faux, and G. D. Landweber, “Spin Holography via Dimensional Enhancement, Phys. Lett. **B681** (2009) 161, arXiv:0907.4543 [hep-th].
- [6] S. J. Gates, Jr., T. Hübsch, and K. Stiffler, “Adinkras and SUSY Holography: Some Explicit Examples, Univ. of Maryland preprint PP-012-019, e-Print: arXiv:1208.5999 [hep-th].
- [7] S. J. Gates, Jr., T. Hübsch, “On Dimensional Extension of Supersymmetry: From Worldlines to Worldsheets,” Univ. of Maryland preprint UMDEPP-011-005, MIT Preprint MIT-CTP-4232, e-Print: arXiv:1104.0722 [hep-th], submitted to Adv. in Theor. and Math. Phys.

- [8] C. F. Doran, M. G. Faux, S. J. Gates, Jr., T. Hubsch, K. M. Iga, and G. D. Landweber, “Relating Doubly-Even Error-Correcting Codes, Graphs, and Irreducible Representations of N-Extended Supersymmetry,” in “Discrete and Computational Mathematics,” p. 53–71, eds. F. Liu et al., (Nova Science Pub., Inc., Hauppauge, 2008), e-Print: arXiv:0806.0051 [hep-th].; C. F. Doran, M. G. Faux, S. J. Gates, Jr., T. Hubsch, K. M. Iga, G. D. Landweber, and R. L. Miller, “Codes and Supersymmetry in One Dimension,” Univ. of Maryland preprint UMDEPP-008-010, State University of New York - Oneonta SUNY-O-667 e-Print: arXiv:1108.4124 [hep-th], to appear in Adv. in Theor. and Math. Phys. **15.6** ; S. J. Gates, Jr., J. Hallett, T. Hubsch, and K. Stiffler, “The Real Anatomy of Complex Linear Superelds,” Univ. of Maryland preprint UMDEPP-012-003, e-Print: arXiv:1202.4418 [hep-th], to appear in the Int. Journ. of Mod. Phys.
- [9] Keith Burghardt, “Less is More,” Univ. of Maryland preprint PP-012-017, in preparation.
- [10] C. F. Doran, M. G. Faux, S. J. Gates, Jr., T. Hubsch, K. M. Iga, and G. D. Landweber, “On the matter of N=2 matter,” Phys. Lett. **B659** (2008) 441, e-Print: arXiv:0710.5245 [hep-th].
- [11] S. J. Gates Jr., J. Gonzales, B. MacGregor, J. Parker, R. Polo-Sherk, V. G. J. Rodgers, and L. Wassink, “4D N = 1 Supersymmetry Genomics (I),” JHEP **12** (2009) 008, [hep-th/0902.3830v4].
- [12] J. Parker, “Diamonds and Bowties: Supersymmetric Graph Conditions,” 2011, unpublished.
- [13] T. Buscher. U. Lindström and M. Roček, “New supersymmetric sigma models with Weaa-Zumino terms,” Lett. Lett. **B202** (1988) 94.
- [14] A. Sevrin, and J/ Troost, “Off-shell formulations of N = 2 nonlinear semi-chiral superfields, Nucl. Phys. **B492** (1997) 623.
- [15] J. Bogaerts, A. Sevrin, S. van der Loo, and S. Van Gil, “Properties of semi-chiral superfields,” Nucl. Phys. **B562** (1999) 277.